Characterization of phenolic compound-modified alpha-2-macroglobulin *in vitro*

Submission by

Em-J Hillman

Supervisors

Dr Amy Wyatt and Dr Noralyn Mañucat-Tan

Submitted 15/11/2023

TABLE OF CONTENTS

LIST OF ABBREVIATIONS

2-mercaptoethanol (2-ME)

4-(2-hydroxyethyl)-1-piperazineethanesulfonic acid (HEPES)

4,4’-bis(1-anilino-8-naphthalene sulfonate) (bisANS)

4,4'-Dianilino-1,1'-Binaphthyl-5,5'-Disulfonic Acid, Dipotassium Salt (bis-ANS)

Absorbance (A)

Active fluorescence units (AFU)

Alpha-2-macroglobulin (α_2M)

Alpha-2-macroglobulin like-1 (α_2ML-1)

Alpha-macroglobulin (αM)

Amino acid (aa)

Ammonium Chloride (NH_4Cl)

Ammonium persulfate ($(NH_4)_2S_2O_8$)

Amyloid-beta (Aβ)

Bovine serum albumin (BSA)

Caffeic acid (CA)

Cerebral spinal fluid (CSF)

Chronic obstructive pulmonary disease (COPD)

Degree Celsius (°C)

Deoxyribonuclease I (DNAse1)

Dialysis control (DC)

Disodium phosphate (Na_2HPO_4)

Dulbecco's Modified Eagle Medium: Nutrient Mixture F12 (DMEM-F12)

Escherichia coli (*E. coli*)

Ethylenediaminetetraacetic acid (EDTA)

Fluorescein isothiocyanate-area (FITC-A)

Foetal bovine serum (FBS)

Grams per mole (g/mol)

Hanks' Balanced Salt Solution (HBSS)

Horseradish peroxidase (HRP)

Human serum albumin (HSA)

Hydrochloric acid (HCl)

Immunoglobulin G (IgG)

Isopropyl β- d-1-thiogalactopyranoside (IPTG)

Kilo Dalton (kDa)

Low-density lipoprotein receptor protein 1 (LRP-1)

Luria-Bertani (LB)

Macroglobulin Activated for Cytokine binding (MAC)

Microgram (µg)

Microlitres (µl)

Micromolar (µM)

Milligram (mg)

Millilitres (ml)

Millimolar (mM)

Nanogram (ng)

Nanometre (nm)

Optical density (OD)

osteoarthritis (OA)

Phosphate-buffered saline (PBS)

Phosphate-buffered saline with tween 20 (PBS-T)

Platelet-rich plasma (PRP)

Polyacrylamide gel electrophoresis (PAGE)

Potassium chloride (KCl)

Potassium phosphate monobasic (KH2PO4)

Pregnancy zone protein (PZP)

Receptor-associated protein tagged with glutathione S-transferase (GST-RAP)

Recombinant bait region mutant (*r*α_2M)

Relative centrifugal force (x g)

Revolutions per minute (rpm)

Rosmarinic acid (RA)

Salvianolic acid β (Saβ)

Size exclusion chromatography (SEC)

Sodium azide (Az)

Sodium chloride (NaCl)

Sodium dodecyl sulfate (SDS)

Sodium hydroxide (NaOH)

Sodium hypochlorite (NaOCl)

Streptavidin (STR)

Streptavidin-Alexa Fluor 488 (STR-488)

Synovial fluid (SF)

Tetramethylethylenediamine (TEMED)

Thioflavin-T (ThT)

Trizma base (Tris)

Zinc affinity chromatography (ZAC)

ABSTRACT

Alpha-2-macroglobulin (α_2M) belongs to the alpha-macroglobulin family of secreted proteins and is constitutively abundant in human biological fluids. The functions of α_2M are dependent on its conformation, which can be native, transformed, or dimeric. Each conformation is functionally distinct, all playing a crucial role in the regulation of inflammatory and immune responses. It has been demonstrated that dissociation of the native α_2M tetramer into dimers is induced by hypochlorite, an inflammatory oxidant, that significantly enhances the holdase-type chaperone activity of α_2M. Preliminary investigations by the Wyatt laboratory identified that phenolic compounds such as rosmarinic acid (RA), caffeic acid (CA) and salvianolic acid β (Saβ), induce α_2M to dissociate into dimer-like molecules. The purpose of this study was to demonstrate the effect of a drug or drug-like phenolic compounds on the conformation of α_2M and compare this to the effect of hypochlorite.

Considering the superior chaperone activity of dimeric α_2M compared to native and transformed α_2M tetramers, this study undertook a series of experiments to characterise the structure and function of phenolic compound-treated α_2M in order to generate proof-of-principle data, to demonstrate whether phenolic compounds could be used to target the chaperone activity of α_2M. Specifically this study aimed to characterise in the holdase-type chaperone activity and cell surface receptor binding of phenolic compound-modified α_2M. The evaluation of holdase-type chaperone activity involved conducting a Thioflavin T (ThT) assay with the Alzheimer's disease-related amyloid beta peptide, $A\beta_{1\text{-}42}$. Assessment of cell surface binding of biotinylated phenolic compound-modified α_2M was accomplished through flow cytometry, utilizing SH SY5Y

neuroblastoma cells. The structural characterization of phenolic compound-modified α_2M included native gel electrophoresis and a bis-ANS assay to analyse migration patterns and surface exposed hydrophobicity, respectively. The proof-of-principle data generated in this study support the conclusion that although phenolic compound-modified α_2M enhanced the ability of α_2M to stabilise $A\beta_{1-42}$, this effect does not occur via a canonical holdase chaperone action. The results also suggest that phenolic compounds may induce a slightly transformed conformation in α_2M, which is electrophoretically fast but shields the hydrophobic regions that are normally exposed on α_2M dimers. The findings support the idea that treatment of α_2M with phenolic compounds may expose the internal thiol ester that forms a covalent bond with $A\beta_{1-42}$ and exposes the LRP-1 binding domain. However additional studies are required to confirm this model.

A greater understanding to the functions of phenolic compound-modified α_2M has the potential to lay the groundwork for developing treatments for conditions characterized by protein misfolding and inflammation.

ELECTRONIC DECLARATION

I certify that this thesis does not contain material which has been accepted for the awards of any degree or diploma; and to the best of my knowledge and belief it does not contain any material previously publish or written by another person except were due reference is made in the text of this thesis.

Emma-Jean Hillman

ACKNOWLEDGEMENTS

I'm grateful for the guidance and support from my supervisors, Dr Amy Wyatt and Dr Mañucat-Tan, for the time and effort they have put in to helping me throughout the duration of this project. I started this project with no background knowledge of this protein or its role. I also had very little to no knowledge of the majority of the techniques that I would end up performing as part of this project. Their patient guidance and instruction were invaluable.

I would also like to extend my thank to Demi Georgiou for her advice and assistance regarding methods and equipment use. In addition, her contribution of biotinylated GST-RAP to my project, which allowed me to complete my flow cytometry experiment.

I would like to acknowledge and extend my thank to Dr Jordan Cater (University of Wollongong) who kindly donated the GST-RAP plasmid DNA used in this study.

I would also like to acknowledge and extend the Briony Laboratory (Flinders University) for their kind donation of the BL21 cells. I would also like to thank them for their allowing me to use their laboratory facility for production of the recombinant GST-RAP, as well as their time and guidance.

Finally, I express my gratitude to Angela Binns, Elise Tucker, Nusha Chegeni, and Dr. Giles Best for training, support in equipment usage, and guidance provided throughout this project.

1 INTRODUCTION

1.1 Overview

Alpha-marcoglobulins (αMs) are a multifunctional protein family that are secreted into biological fluids. Alpha-2-macroglobulin (α_2M) is the predominant αM protein in human and is constitutively abundant. α_2M is a tetramer with two distinct conformations, these involve a native conformation exhibiting broad-spectrum anti-protease activity and a transformed "compact" conformation that modulates signalling pathways (Sun *et al*., 2023; Lindner *et al*., 2010) and aids in bacterial clearance (Godehardt *et al*., 2004; De Boer *et al*., 1993). The native α_2M tetramer can be induced to dissociate into functionally distinct dimers, which have been shown to possess enhanced holdase-type chaperone activity *in vitro* (Wyatt *et al*., 2014).

Due to its diverse functional conformations, α_2M has been suggested as a tractable therapeutic target in the treatment of several diseases related to inflammation and protein misfolding, and numerous therapeutic opportunities have been explored (Wang *et al*, 2014., Tavassoli *et al*, 2019., Louis *et al*, 2021., Ikai *et al*, 1999., Harwood *et al*, 2021). However, to date, there is no clinical strategies specifically targeting the functions of α_2M. Instead, current therapies focus on increasing local native α_2M concentrations at the site of inflammation (Wang *et al*., 2014) or generating a pool of transformed α_2M in systemic circulation (Desser *et al*., 2001).

Exploring the use of drug and drug-like compounds has also been investigated as an approach to influence α_2M conformations in systemic circulation. Preliminary studies from the Wyatt laboratory, identified that phenolic compounds such as caffeic acid (CA), rosmarinic acid (RA) and

salvianolic acid β (Saβ), induce the native α_2M tetramer to dissociate into dimer-like molecules. Phenolic compound-modified α_2M migrates in native gel electrophoresis similar to holdase-type chaperone active hypochlorite-modified α_2M dimers (Georgiou *et al*., unpublished data).

The current study extends on these preliminary findings to further characterise the structure and function of phenolic compound-modified α_2M to generate proof-of-principle data that demonstrates the effect of phenolic compounds on the chaperone activity and cell surface binding of α_2M.

1.2 Alpha-macroglobulin protein family

αM proteins can be monomers (i.e. alpha-2-macroglobulin like-1; α_2ML-1), dimers (i.e. Pregnancy zone protein; PZP) or tetramers (i.e. α_2M). Several αM proteins can function as protease inhibitors by trapping proteases after they cleave the protease-sensitive bait region. The length and sequence of the bait region exhibits high variability among αM family members and determines the substrate specificity of αM protease inhibitors. In addition, the quaternary structure of αM protein (i.e. tetrameric, dimeric or monomeric) greatly effects its efficiency to trap proteases. This is because, upon cleavage of the bait region by a protease, a conformational change is initiated, leading to a more compact "transformed" conformation that encloses on the protease (Sand *et al*., 1985) and in so doing, physically blocks the interaction between proteases and their macromolecular substrates.

1.3 Alpha-2-macroglobulin

1.3.1 Structure

Native α_2M is a tetramer of 720 kDa that is composed of four identical highly glycosylated monomeric subunits (180 kDa). Each monomer is 1451 amino acid residues in length and contains sequences for a bait region, reactive internal β-cysteinyl-γ-glutamyl thiol ester bond, receptor binding site for low density lipoprotein receptor-related protein-1 (LRP-1), and a number of conserved macroglobulin domains (Figure 1). Native α_2M is formed after two monomers are disulfide-linked to form a dimer and then two disulfide-linked dimers non-covalently associate to complete the quaternary structure (Figure 1). Thus, the native α_2M tetramer may be considered a dimer of dimers.

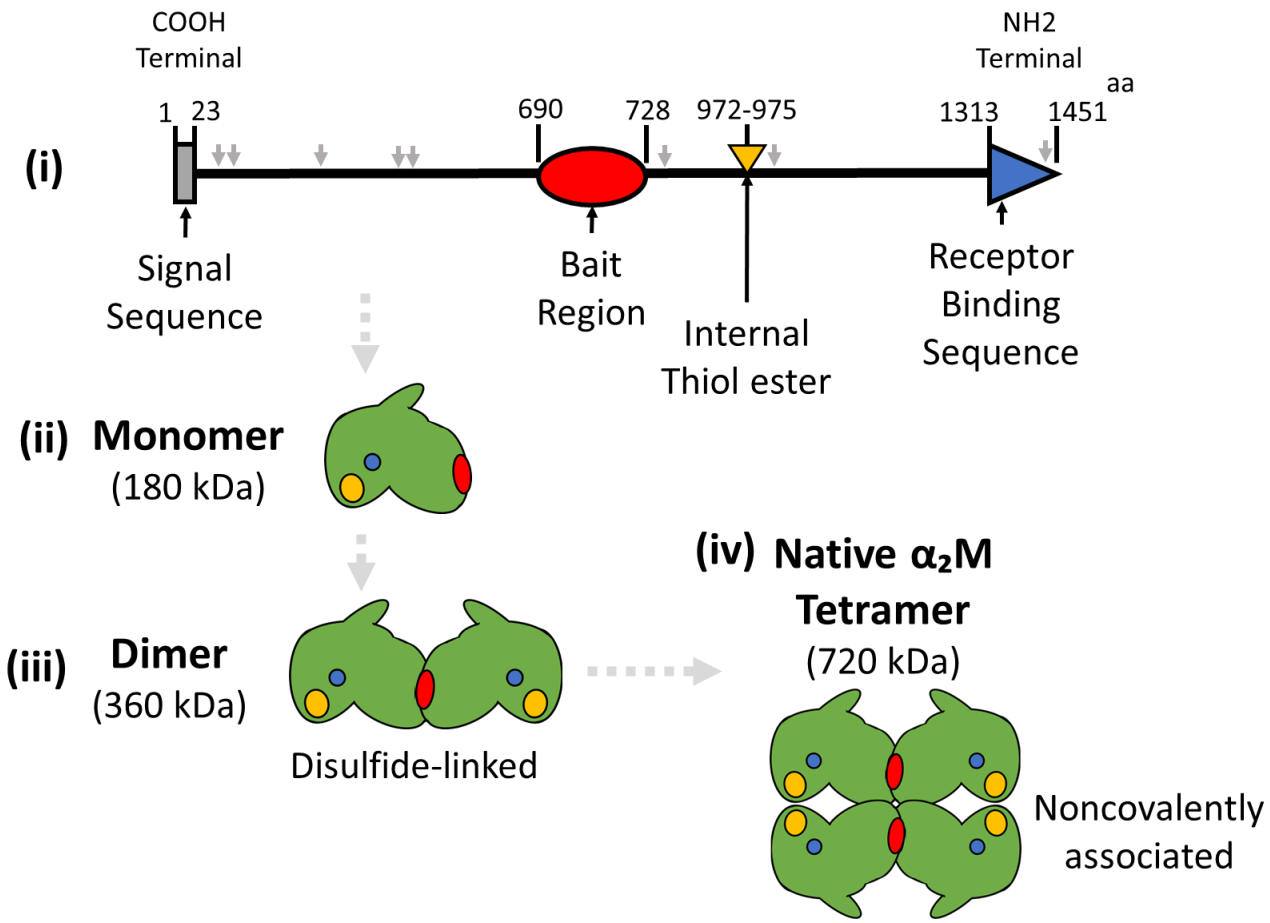

Figure 1. Domain and quaternary structure of α_2M. (i) Diagram of the functional domains of α_2M including signal sequence, bait region, internal thioester and receptor binding site as indicated. N-glycosylation sites are indicated by grey arrows in the monomeric aa sequence. (ii) Schematic representation of an α_2M monomer. Approximate location of bait region (red), thiol ester (yellow) and receptor binding site (blue) are illustrated. Two monomers are connected by disulfide-bridges to form a dimer (iii) and two dimers are noncovalently associated to form the native α_2M tetramer (iv). Illustrations of the α_2M quaternary structure are based on the crystal structure of human α_2M by Huang *et al* (2022).

1.3.2 Expression and Tissue distribution

α_2M is a highly abundant protein in human biological fluids and constitutes a significant portion of the protein component of blood plasma. α_2M in circulation is primarily synthesised by hepatocytes (Petersen *et al*, 1988), but can be synthesised by many other cell types including fibroblasts (White *et al*, 1980) and lymphocytes (Michelis *et al*, 2022).

In children aged up to three years, plasma α_2M levels typically range from 4-5 mg/ml and tend to steadily decrease to 2-4 mg/ml in early adulthood (Ganrot and Schersten, 1967). As individuals age, α_2M levels continue to decrease steadily and by the age of 50, α_2M levels typically range between 1.0-2.5 mg/ml, with lower levels measured in men than women (Ganrot and Schersten, 1967). On the other hand, α_2M level in cerebral spinal fluid (CSF) increase with age. In healthy individuals under the age of 50, α_2M levels typically range from 1.0-2.5 µg/ml. While for individuals over 50 years old, the range of α_2M levels extends to 2.0-3.6 µg/ml (Garton *et al,* 1991).

Conditions such as type 2 diabetes and Alzheimer's are reportedly associated with increased plasma α_2M concentrations (Tariq *et al*, 2022., Varma *et al,* 2017). This systemic increase in α_2M circulation is also observed in certain chronic inflammatory conditions such as chronic obstructive pulmonary disease (COPD) (Xiao *et al*., 2023). Interestingly, while systemically α_2M concentrations are increased, the localized concentration of α_2M at sites of localised inflammation may shows a notable reduction (Xiao *et al*., 2023).

Elevations in α_2M concentration has also been reported in other bodily fluids in the presence of disease. For example, a study by Wang *et al* (2014) reported that the synovial fluid (SF) of healthy

individuals typically exhibit α_2M concentrations of 126 µg/ml, whereas in individuals with osteoarthritis (OA) SF, the concentration increases almost 2-fold to approximately 240 µg/ml.

α_2M is also present in ocular fluid and can be produced by endothelial cells in the human eye choroid. Disease-specific patterns have also been noted in tear fluid, which is produced from this ocular fluid, with α_2M concentration observed to be 1.5 times higher in patients diagnosed with Parkinson's disease compared to controls (Boerger *et al*, 2019). However, it's unclear how much of the concentration of α_2M in this fluid originates from cellular expression and how much comes from plasma α_2M that has entered the ocular fluid.

1.3.3 Function

α_2M is a highly efficient protease inhibitor and is unique in its ability to bind to all four classes of endogenous proteinases in humans (Sottrup-Jensen *et al*, 1989). After the bait region is cleaved by a protease, a conformational change occurs and α_2M adopts a more compact "transformed" conformation where the four subunits enclose and form a steric cage around the protease. This conformational change exposes the internal thiol ester which forms a covalent bond between the α_2M molecule and protease (Figure 2) (Harwood *et al*, 2022., Huang *et al*, 2022).

Transformed α_2M can also bind non-covalently to a large number of ligands, as well as misfolded proteins. This non-covalent binding to ligands has an important functional role in regulating immune responses and inflammation through mediating cell signalling pathways (Zhu *et al*, 2021., Kardas *et al*, 2020). Specifically, many cytokines and growth factors can bind to transformed α_2M conformation (Crookston *et al*, 1993) and by binding to these ligands,

transformed α_2M can influence the strength and duration of many signalling pathways by preventing these molecules from binding to their receptors (Sun *et al*, 2023., Lindner *et al*, 2010). Through these interactions α_2M can modulate several important processes including cell proliferation, migration, and immune responses.

The conformational change resulting from the trapping of proteases, also exposes the receptor binding site for low-density lipoprotein receptor-related protein-1 (LRP-1) and allows for rapid clearance of the α_2M-protease complex and any non-covalently bound ligands by endocytosis (Huang *et al*, 2022). LRP-1 is expressed on multiple cell types including hepatocytes, macrophages, adipocytes, fibroblasts, dermal dendritic cells, and syncytiotrophoblasts (Chiabrando *et al*., 2002).

During inflammation, native α_2M tetramers can be induced to dissociate into dimers. This process is regulated by the production of hypochlorite, a potent inflammatory oxidant generated by the enzyme myeloperoxidase. Hypochlorite is thought to induce dissociation into dimers by rapidly reacting with a series of methionine residues between the non-covalently associated disulfide-linked α_2M dimers (Reddy *et al*, 1994). The separation of the two disulfide-linked α_2M dimers exposes the hydrophobic region which is normally protected in the native α_2M conformation (Figure 2) (Wyatt *et al*, 2014). In addition, the receptor binding site for LRP-1 also becomes exposed in the induced dimeric conformation (Wyatt *et al*, 2014). Dimeric α_2M is functionally distinct from the native and transformed α_2M tetramer, in that there is enhanced holdase-type chaperone activity resulting from the highly exposed hydrophobic region (Figure 2) and preferentially binding of several pro-inflammatory molecules including TNF-α, TNF-β and IL-6

(Wyatt *et al*, 2014., Wu *et al*, 1998). As such it has been proposed that hypochlorite-induced dissociation α_2M is a rapid response that controls the accumulation of misfolded proteins and inflammation during acute stress (Wyatt *et al*., 2014). But it is currently unknown whether or not this property of α_2M could be targeted therapeutically.

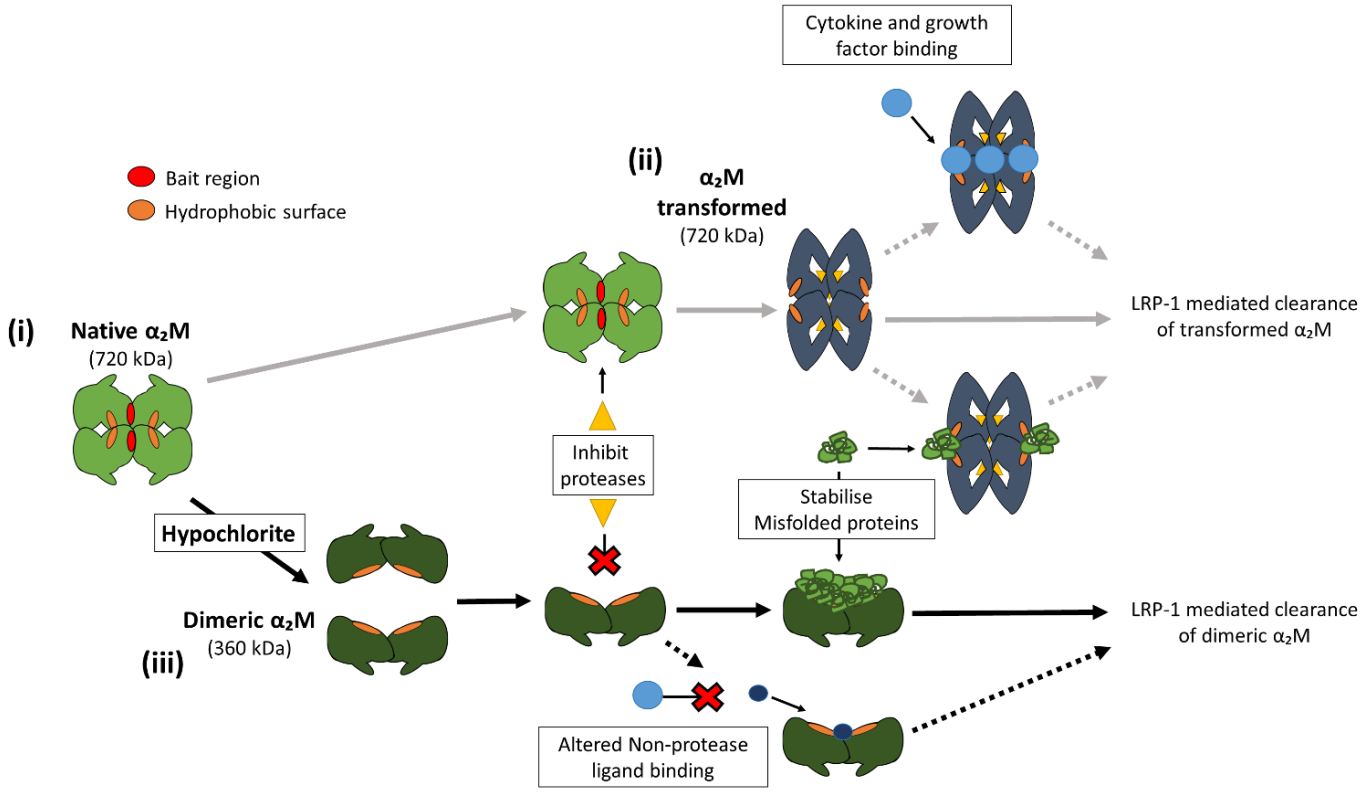

Figure 2. Schematic diagram showing conformation specific functions of α_2M. (i) Native α_2M showing the flexible surface exposed bait region and hydrophobic interface that is normally concealed. When a protease cleaves the bait region, a conformation change occurs and α_2M adopts a more compact transformed conformation (ii). Transformed α_2M can bind non-covalently to a large number of ligands and has limited holdase-type chaperone activity. Hypochlorite potently induces dissociation of the native α_2M tetramer (i) into dimers (iii). Dimeric α_2M loses ability to inhibit proteases but binds to a large number of non-covalent ligands. Reaction with hypochlorite exposes the normally protected hydrophobic region and allows for enhanced holdase-type chaperone activity. In both transformed α_2M and hypochlorite-

modified α_2M dimers, the receptor binding site for LRP-1 is exposed and mediates the clearance of α_2M and its cargo.

1.4 Therapeutic opportunities

1.4.1 Proteolytic- enzyme therapy

Proteolytic-enzyme therapy, a form of systemic enzyme therapy, involves the administration of proteolytic enzymes into the body through oral or intravenous delivery. While this form of therapy was initially used to increase proteolytic-enzyme activity *in vivo*, other therapeutic opportunities were quickly identified including using this approach to increase the pool of transformed α_2M present in blood.

As previously discussed, transformed α_2M is generated when native α_2M traps proteases and a conformational change occurs where the protein adopts a more compact conformation (Figure 2). Consequently, an increase in systemic levels of proteases, elevates the concentration of transformed α_2M present in circulation. As transformed α_2M is known to bind to pro-inflammatory cytokines and growth factors this form of therapy offers potential benefits in helping reduce inflammation.

Desser *et al* (2001) proposed that oral administration of proteolytic enzymes (papain, bromelain, trypsin, and chymotrypsin) reduced TGF-β levels in human blood, as a result of the increased transformed α_2M in circulation. When patients with excessive TGF-β levels (>50 ng TGF-β/ml serum) were provided with proteolytic enzyme therapy, the researchers observed a significant

reduction (P<0.005) in TGF-β levels in the blood from 67.84 +/- 24.81 ng/ml serum to 8.11+/- 29.49 ng/ml serum.

Other published research supports that oral administration of proteases increases the circulating pool of transformed α_2M (Leipner and Saller, 2001) and that *in vitro*, transformed α_2M can non-covalently bind to TGF-β. However, there is currently no data demonstrating that transformation of α_2M directly underpins the reduction in TGF-β.

Despite this, proteolytic-enzyme therapy has been proposed as a complementary strategy in the treatment of cancer and other pathologies (reviewed in Gremmler *et al*, 2021). While systemic enzyme therapy is not a new approach, its application in treatment of inflammation and immune response continues to evolve.

1.4.2 Autologous α_2M administration

Autologous administration refers to a medical procedure where a patient's own biological materials, such as blood, are collected, processed, and then reintroduced into the same patient's body for therapeutic or diagnostic purposes. For α_2M, the process involves concentrating this protein from the patient's blood plasma or serum. This concentrated α_2M is then injected into joints, especially in conditions where excessive protease activity, such as in osteoarthritis (OA), is a contributing factor (reviewed in Troeberg and Nagase, 2012). The aim of this therapy is to utilise α_2M to inhibit the activity of destructive proteases, particularly when uncontrolled protease activity leads to tissue damage, inflammation, or degenerative conditions.

The current evidence regarding the use of concentrated α_2M injections for treating OA primarily relies on animal models. However, these models suggest that administering concentrated α_2M into knee joints has the potential to significantly decrease levels of inflammatory infiltration and alleviate cartilage and bone damage (Wang *et al*, 2014). This approach shows potential for OA treatment. However, it's important to note that there are certain limitations when it comes to its clinical application. Notably, the studies use $_{\alpha 2}$M purified from human serum, a process that can be time-consuming and expensive.

As an alternative approach, rather than the purification and concentration of α_2M, blood plasma, which contains other highly beneficial components in addition to α_2M, can be concentrated into platelet-rich plasma (PRP). This method offers an alternative strategy for harnessing the therapeutic potential of these naturally occurring components.

Clinical studies suggest that injecting platelet-rich plasma (PRP), where concentrated α_2M is a key component in this considering it abundance in blood plasma, seems to alleviate osteoarthritis symptoms and stimulate cartilage growth (Tavassoli *et al*, 2019., Louis *et al*, 2021). However, an important consideration is the limited current studies and mixed evidence of effectiveness of this therapy that is dependent on the measurement system used for assessing efficacy and response to treatment (Di *et al*, 2018). With five different scoring systems currently accepted including Western Ontario and McMaster Universities Osteoarthritis Index (WOMAC), International Knee Documentation Committee (IKDC), Knee Injury and Osteoarthritis Outcome Score (KOOS), EuroQol visual analogue scale (EQ VAS) and Tegner score. But as highlighted by Di *et al* (2018) systematic review of randomized controlled trials that used these different scoring systems, PRP

that contained concentrated plasma α_2M was only found effective when using WOMAC to define efficiency and response to treatment. In addition, there another limitation is the ambiguity in defining PRP, with the concentration of α_2M undetermined but assumed to be increase as the plasma is concentrated.

Autologous administration of plasma rich in α_2M is a novel therapy with the potential for significant therapeutic opportunities. Concentrating plasma proteins such as α_2M is relatively low-cost, minimally invasive and eliminates risk of rejection. But requires further investigation to determine actual therapeutic benefits *in vivo*.

1.4.3 Recombinant bait region mutant α_2M

Recombinant technologies enable the generation of α_2M with purposeful genetic modification to alter the bait region and thereby expand or narrow α_2M's protease trapping ability. For the purposes of this thesis, recombinant α_2M bait region mutant was abbreviated to *r*α_2M in this section. The bait region in α_2M, which is a 38-amino acid sequence , plays a crucial role in protease inhibition. As previously established, α_2M is distinctive among protease inhibitors due to its capacity to bind to virtually all known proteinases in humans. Nonetheless, there are certain proteases produced by microorganisms that are not completely inhibited or only partially inhibited by human α_2M. For example, proteases produced by *Clostridium perfringens* (Wolf *et al*., 1992), and *Serratia liquefaciens* (Wolf *et al*., 1991). *Achromobacter lyticus* lysyl endopeptidase is an example of a protease produced by a microorganisms that are not completely inhibited by

α_2M. This is thought to be due to lysyl endopeptidase requiring a lysyl residues in the bait region to be cleave (Sakiyama and Masaki, 1994), which human α_2M lacks.

Early studies in *r*α_2M intended to investigate whether mutation in the bait region could expand the types of proteases that α_2M could inhibit while maintaining its original inhibitory activity of human α_2M. In the study by Ikai *et al* (1999), they effectively engineered *r*α_2M by replacing an Arginine codon with a lysine codon. They discovered that the *r*α_2M with the lysine codon could inhibit *Achromobacter lyticus* lysyl endopeptidase protease activity, unlike the wildtype human α_2M. Interestingly, while mutations at two different locations for lysine codon mutation at either codon 692 or 696 were made, only the mutation at codon 696 exhibited any inhibitory activity (Ikai *et al*, 1999). However, this inhibitory effect was only partial and inefficient as it required 5 to 10 times molar excess of the *r*α_2M over lysyl endopeptidase to observe the reported inhibitory activity (Ikai *et al*, 1999). Moreover, mutations at both codon locations for *r*α_2M decreased the inhibitory efficiency of other proteases such as trypsin by *r*α_2M.

More recently, the emphasis of *r*α_2M studies has shifted towards modifying human α_2M to possess targeted protease inhibitory capabilities rather than broadening its scope. In a study by Harwood *et al* (2021), they engineered an *r*α_2M featuring a repetitive glycine-serine codon sequence in the bait region, this sequence, when tested against 12 proteases, showed no activity.

By inserting an appropriate cleavage site into this sequence, selective protease inhibitory activity against trypsin was demonstrated (Harwood *et al*, 2021). Yet, a notable limitation of this approach was highlighted as a result of this study, in that some proteases do not have a specific sequence that would allow for selective binding. This was demonstrated in the study by Harwood

et al (2021), for MMP2 substrate sequences within the human α_2M bait region, which instead revealed sequences that generically cleaved MMP motifs. Although this generic sequence makes the α_2M bait region highly effective in cleaving multiple proteases within a motif, it limits the potential for engineering α_2M for specific proteases within a motif. Nevertheless, artificially altering proteinase inhibitory spectrum still would offer a wide range of potential applications, including significant research and therapeutic purposes, with the ability to expand or narrow inhibitory activity of this protein to specific proteases and their motifs.

1.4.4 Drug-induced alternative conformation of α_2M

Considering that numerous functions of α_2M are dependent on specific conformations, an intriguing avenue of research involves the identification of drugs or drug-like compounds capable of inducing alternative conformations in α_2M. As discussed earlier, α_2M exhibits various functionally distinct conformations (Figure 2). The induction of alternative conformations in α_2M provides the prospect of broadening the systemic availability of specific protein functions, presenting a potentially novel approach in the treatment of disorders associated with protein misfolding and inflammation.

An early example of this approach involved the use of cisplatin, a chemotherapy medication. Binding of cisplatin to α_2M generates a transformed-like conformation, with this alternative conformation referred to as Macroglobulin Activated for Cytokine binding (MAC). The resulting MAC proteins lost their function in protease trapping but were found to have enhanced binding to TNF-α and IL-1β *in vitro* (Webb and Gonias, 1998., Zia *et al*, 2018). Subsequent investigations

using animal models demonstrated that generation of MAC regulated the inflammatory response of macrophages and proinflammatory cytokines, potentially offering a protective effect on nerve tissue degeneration associated with peripheral nerve injuries (Arandjelovic *et al*, 2007). Interestingly, migration of MAC in native page appears to be modestly faster than native α_2M, but not as fast as transformed α_2M generated by reaction with proteases (Arandjelovic *et al*, 2007). It is thought that cisplatin may be replacing nucleophilic protein groups with platinum (II) from highly stable bonds that lock α_2M into a semi-transformed conformation. Such interactions might restrict the conformational changes of the modified protein and potentially explain the loss of protease inhibitory activity in MAC (Gonias *et al*, 1984).

Recently, the Wyatt laboratory have investigated the potential of several drug compounds including N-acetylcysteine, hydrazine sulfate and several phenolic compounds, to modify the conformation of α_2M (Georgiou *et al*, unpublished data., Saviane *et al*, unpublished data). The results of preliminary studies show that treatment of α_2M with phenolic compounds including caffeic acid (CA), rosmarinic acid (RA) and salvianolic acid β (Saβ) induce the formation of α_2M species that migrate similar to hypochlorite-modified α_2M dimers by native gel electrophoresis (Georgiou *et al*, unpublished data). This observation supports the idea that phenolic compounds may have the potential to unlock the chaperone activity and anti-inflammatory activities of α_2M that are greatest when α_2M is induced to form dimers.

1.5. Phenolic compounds

Phenolic compounds are a diverse group of chemical compounds found abundantly in various plant sources, including fruits, vegetables, whole grains, nuts, seeds, spices, and beverages like tea, coffee, and wine. They are characterised by a phenol group, which consists of an aromatic ring bonded to a hydroxyl group.

Phenolic compounds are known for their diverse biological activities and health benefits (reviewed in Albuquerque *et al*, 2020). CA, RA and Saβ belong to the phenolic compound family of hydroxycinnamic acid compounds. These compounds have a C6-C3 carbon backbone and are derived from cinnamic acid via hydroxylation or methylation.

CA (3,4-dihydroxycinnamic acid; Figure 3) is abundant in various plant sources such as coffee, fruits, and vegetables. It possesses antioxidant properties, helping to combat oxidative stress and free radical damage within the body (Gülçin, 2006., Maurya and Devasagayam, 2010). Additionally, animal models demonstrate anti-inflammatory and neuroprotective effects via modulating signalling pathways (Huang *et al,* 2018., Paciello *et al*, 2020) and synaptic plasticity Chang *et al*, 2019).

RA is found in herbs such as rosemary, oregano, and mint. Chemically, it is formed as an ester of caffeic acid with 3,4-dihydroxyphenyllactic acid (Figure 3). Saβ also contains an CA molecule but with three molecules Danshensu [(R)-3- (3, 4-Dihydroxyphenyl)-2-hydroxypropanoic acid] attached (Figure 3). Saβ is derived from the root of Salvia miltiorrhiza and has been used in traditional Chinese medicines for its benefits in cardiovascular health (reviewed by Chen *et al*,

2017). Both RA and Saβ demonstrate strong antioxidant and anti-inflammatory properties. Similar to CA, animal studies of both RA and Saβ have also show these compounds have a neuroprotective effect, as well as an anticancer effect through modulating signalling pathways (Lv *et al*, 2020., Zhang *et al*, 2018., Mahmoud *et al*, 2021).

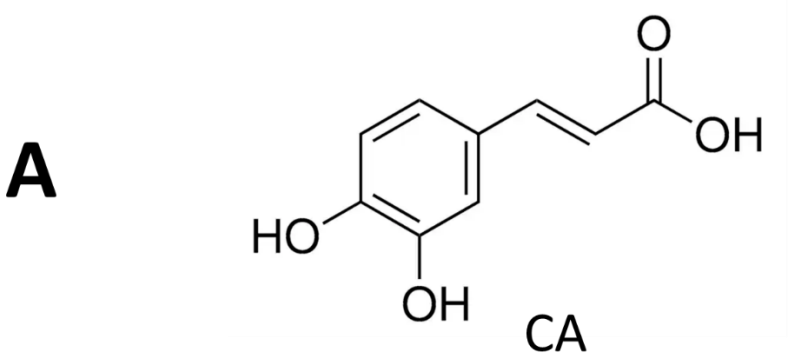

Molecular formular: $C_9 H_8 O_4$

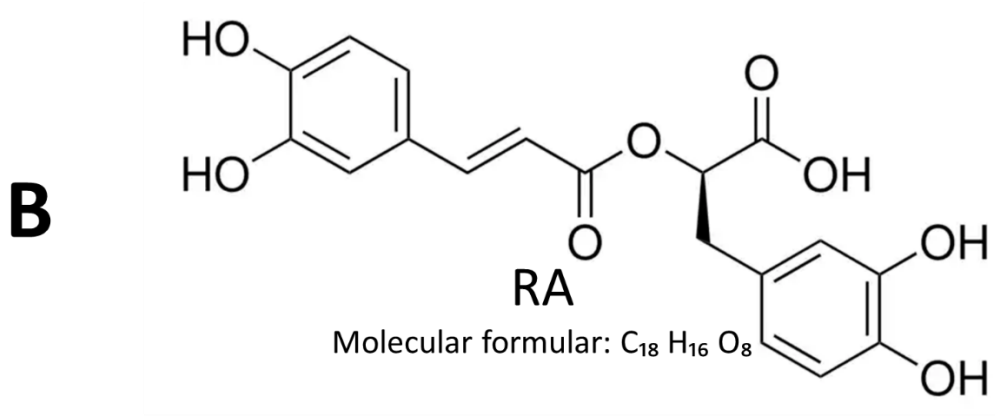

Molecular formular: $C_{18} H_{16} O_8$

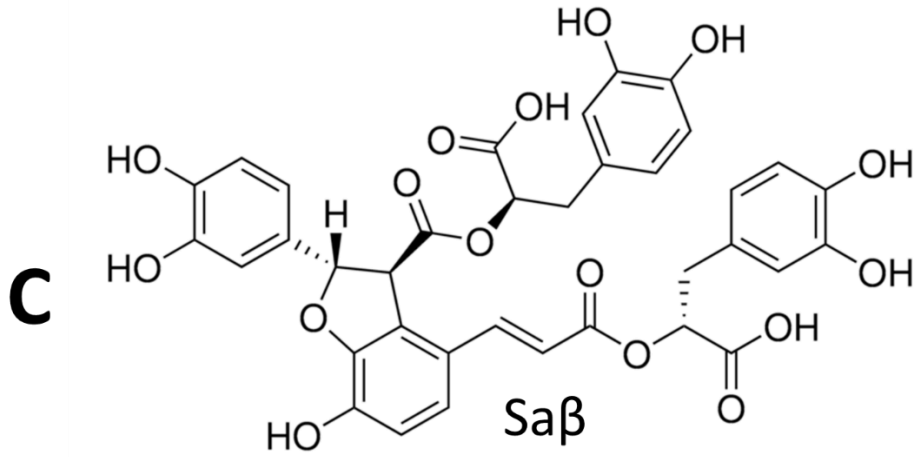

Molecular formular: $C_{36} H_{30} O_{16}$

Figure 3. Chemical structure of (A) CA, (B) RA and (C) Saβ.

1.6 Project Overview

Preliminary studies performed in the Wyatt laboratory have identified that incubation of native α_2M with phenolic compounds including CA, RA and Saβ induce the formation of species that migrate similar to hypochlorite-induced α_2M dimers by native gel electrophoresis (Georgiou *et al*, unpublished data., Saviane *et al*, unpublished data). The purpose of this study is to characterise phenolic compound-modified α_2M and compare its function to that of hypochlorite-modified α_2M. Considering the enhanced chaperone and anti-inflammatory activities of hypochlorite-modified α_2M, the experiments performed in this study are an important first step towards understanding if phenolic compounds might be suitable for targeting these properties of α_2M *in vivo*. In this report phenolic compounds-modified α_2M will be represented by the compound's abbreviation followed by "α_2M." For example, CA-modified α_2M will be abbreviated to CA-α_2M, RA-modified α_2M to RA-α_2M and Saβ-modified α_2M to Saβ-α_2M.

1.6.1 Hypothesis

It is hypothesised that treatment of native α_2M with CA, RA or Saβ will have similar structural and functional consequences to the treatment of native α_2M with hypochlorite *in vitro*.

Specifically, treatment of native α_2M with the aforementioned phenolic compounds will enhance the holdase-type chaperone activity of α_2M and reveal the cryptic binding site for LRP-1.

1.6.2 Project Aims

1. To purify native α_2M from human blood plasma
2. To treat α_2M with CA, RA or Saβ under conditions that induce its dissociation into dimers.
3. To characterise the effect of treatment with phenolic compounds on:
    i. The chaperone activity of α_2M
    ii. The binding of α_2M to the surface of cells expressing LRP-1 *in vitro*.

2 METHODS AND MATERIALS

2.1 Materials and reagents

Table 1. Reagent consumables used in this project.

Reagent	Manufacture
2-mercaptoethanol (2-ME)	Sigma Aldrich
4-(2-hydroxyethyl)-1-piperazineethanesulfonic acid (HEPES)	VWR Chemicals
Acrylamide/Bis-acrylamide, 30% solution	Sigma Aldrich
Alzheimer's disease associated amyloid beta peptide (Aβ1-42)	Thermo Fisher Scientific
Ammonium persulfate ($(NH_4)_2S_2O_8$)	Sigma Aldrich
Ammonium Chloride (NH_4Cl)	Sigma Aldrich
Ampicillin sodium salt	Sigma Aldrich
Biotin	Sigma Aldrich
Bromophenol blue	Sigma Aldrich
Bis-ANS	Thermo Fisher Scientific
Bovine serum albumin (BSA)	Thermo Fisher Scientific
Caffeic acid	Sigma Aldrich
Clarity western ECL substrate luminol/enhancer solution	Bio-Rad
Clarity western ECL substrate peroxide solution	Bio-Rad
Dimethyl sulfoxide	Sigma Aldrich
Dulbecco's-modified eagle medium (DMEM)/F-12 HAM (DMEM-F12)	Sigma Aldrich
Disodium phosphate (Na_2HPO_4)	Sigma Aldrich
Deoxyribonuclease I (DNAse1)	Thermo Fisher Scientific
EDTA-free Complete Protease Inhibitor Cocktail	Sigma Aldrich
Ethanol 100% undenatured	Chem-Supply
Ethylenediaminetetraacetic acid (EDTA)	Sigma Aldrich
Foetal bovine serum (FBS)	Sigma Aldrich
Glutamax	Sigma Aldrich
Glutathione	Sigma Aldrich

Glycerol	Sigma Aldrich
HRP streptavidin	Thermo Fisher Scientific
Imidazole	Sigma Aldrich
InstantBlue Commassie protein stain	abcam
Isopropyl β- d-1-thiogalactopyranoside (IPTG)	Sigma Aldrich
Luria-Bertani (LB) agar powder	Thermo Fisher Scientific
lysozyme	Thermo Fisher Scientific
Luria-Bertani (LB) broth base powder	Thermo Fisher Scientific
Millipore anti amyloid beta WO2	Thermo Fisher Scientific
Magnesium chloride ($MgCl_2$)	Sigma Aldrich
Nutrient Mixture F12 (F12K)	Sigma Aldrich
Potassium chloride (KCl)	Sigma Aldrich
Potassium phosphate monobasic (KH2PO4)	Sigma Aldrich
Precision plus protein dual Xtra standards	Bio-Rad
Rabbit anti-mouse IgG HRP	Thermo Fisher Scientific
Rosmarinic acid (RA)	Sigma Aldrich
Salvianolic acid β (Saβ)	Sigma Aldrich
Skim milk powder	Coles
Sodium azide (Az)	Sigma Aldrich
Sodium chloride (NaCl)	Chem-supply
Sodium dodecyl sulfate	Sigma Aldrich
Sodium hypochlorite (NaOCl)	Sigma Aldrich
Sodium hydroxide (NaOH)	Sigma Aldrich
Streptavidin-Alexa Fluor 488 (STR-488)	Life Technologies
Tetramethyl-ethylenediamine (TEMED)	Sigma Aldrich
Thioflavin T (ThT)	Sigma Aldrich
Triton X-100	Sigma Aldrich
Trizma base (Tris)	Sigma Aldrich
Tween 20	Sigma Aldrich
Zinc sulfate heptahydrate	Sigma Aldrich

Table 2. Material consumables used in this project.

Reagent	Manufacture
NuPAGE 3-8% Tris- Acetate Gel, 1.5mm x 10 wells	Thermo Fisher Scientific
iBlot 2 NC mini stacks	Thermo Fisher Scientific
15 ml centrifuge tubes	Accumax
50 ml centrifuge tubes	Accumax
25cm^2, Cell culture flasks	Cellstar
75cm^2, Cell culture flasks	Corning
Minisart syringe filter 0.22µM	Sartorius
Minisart syringe filter 0.45µM	Sartorius
Terumo syringe without needle, 10cc/ml	Terumo
Terumo syringe without needle, 50cc/ml	Terumo
384-well plate	Thermo Fisher Scientific

2.2 General Methods

2.2.1 SDS-PAGE

Proteins were analysed by sodium dodecyl sulfate (SDS)-polyacrylamide gel electrophoresis (PAGE),

SDS-PAGE involved dilution of the proteins in a 4x denaturing loading buffer (200mM Tris, 40% (w/v) glycerol, 2% (w/v) SDS, 0.4% (w/v) bromophenol blue, pH 6.8) and electrophoresis using 1.5mm hand cast 8% Tris-HCl gel in Tris-glycine SDS running buffer (250mM Tris, 14.4% (w/v) glycerol, 1% (w/v) SDS). Running time for 15-minutes at 90V, followed by 1-hour at 120V. See Appendix Section 7.1.1 for protocol on hand casting SDS-PAGE gels.

In some experiments, proteins were reduced by incubating them with 7% (v/v) 2-mercaptoethanol (2-ME) at room temperature for 5-minutes prior to electrophoresis.

Protein size was estimated using precision plus protein dual Xtra standards. All gels were stained with InstantBlue for 30-minutes and subsequently detained with MilliQ H_2O. Stained gels were images using a GelDoc imaging system (Bio-rad).

2.2.2 Native-PAGE

For proteins over 250 kDa (i.e. α_2M), samples were diluted using a 4x native loading buffer (200mM Tris, 40% (w/v) glycerol, 0.4% (w/v) bromophenol blue, pH 6.8) and electrophoresed using NuPAGE 3-8% Tris-Acetate gel (precast) in native Tris-glycine running buffer (250mM Tris, 14.4% (w/v) glycerol) at 150V for 90-minutes in a XCell Surelock mini-cell system (Thermo Fisher Scientific). All native gels were stained and imaged as described in section 2.2.1.

2.2.3 Western Blot

For Western blot analysis, proteins separated by native or SDS-PAGE were transferred to a nitrocellulose membrane using iBlot 2 transfer system (Thermo Fisher Scientific). See Appendix Section 7.1.2 for transfer method.

The membrane was then blocked overnight at 4°C in phosphate-buffered saline with tween 20 (PBS-T; 1.37M NaCl, 27mM KCl, 100mM Na_2HPO_4, 18mM KH_2PO_4, 1% (v/v) tween 20) containing 10% (w/v) skim milk and 0.01% (w/v) sodium-azide (Az). Proteins of interest were subsequently

probed using the primary antibodies (Table 3). Typically, the membrane was incubated for 1-hour at room temperature with gentle shaking. The binding of the primary antibody was detected by incubating the membrane with a highly cross-absorbed horseradish peroxide (HRP)-conjugated secondary antibody (see Table 3) for 1-hour at room temperature with gentle shaking. Between each step membranes were washed in PBS-T for 30-minutes. For imaging, bands were visually enhanced with Clarity western ECL substrate (1:1 (v/v) luminol/enhancer solution to peroxide) and imaged using a Chemidoc imaging system (Bio-Rad). All antibodies were diluted at concentrations of 1:1000 – 1:2000, according to the specific manufacturer instructions.

Alternatively, protein samples were directly pipetted onto nitrocellulose membrane (0.2 µM pores) and allowed to dry before blocked and probed following the same methods as the Western blotting.

Table 3. Antibodies used in analysis in Western blotting. Lists the primary and corresponding secondary antibody with there usage or purpose in this study.

Primary Antibody	Secondary Antibody	Usage/Purpose
-	HRP-conjugated Streptavidin (STR-HRP)	Used for detection of biotinylated proteins. To determine if proteins are successfully biotinylated.
Anti-amyloid β, clone W0-2	Rabbit Anti-mouse HRP Polyclonal (IgG)	Used for detection of Aβ1-42 detection.

2.2.4 Protein Quantification

2.2.4.1 Protein concentration

To assess the amount of protein within samples, protein concentrations were estimated by measuring the absorbance at 280nm (A_{280}) using a Nanodrop 2000C (Thermo Fisher Scientific). All measurements were adjusted using the appropriate blank and measured in triplicate. The concentration of the proteins was then calculated using the extinction co-efficient (Table 4).

Table 4. Values for quantification of proteins used in this project. Dimeric α_2M in this instance refers to both the hypochlorite and phenolic compound-modified α_2M proteins.

Proteins	Absorbance (1 mg/ml)	Molecular weight (g/mol)
α_2M	0.89	720,000
Dimeric α_2M	0.89	360,000
GST-RAP	1	64,000

2.2.4.2 Densitometry

As a crude measure of the percentage of proteins in the bands of native or SDS gels, densitometry analysis was performed using the Gel Analyzer tool on Image J image processing software.

2.3 α_2M Purification

α_2M purification involved two parts; (1) preparation of the blood plasma and (2) eluting of putative α_2M via zinc affinity chromatography (ZAC).

2.3.1 Preparation of blood plasma

Human blood (~100 ml) was collected from a healthy consenting donor in lithium heparin blood collection tubes at SA Pathology, Flinders Medical Centre by a phlebotomist. The blood was immediately centrifuged (1300 x g, 10 minutes, 4°C) and the plasma was collected. The plasma (~45 ml) was then supplemented with 1M NaCl, 20 mM HEPES (pH 7.4) and EDTA-free Complete Protease Inhibitor Cocktail and filtered (0.45 µM syringe filter).

2.3.2 Zinc affinity chromatography (ZAC)

Human plasma (as prepared in 2.3.1) was loaded onto a HiTrap chelating HP column (GE Healthcare) using a Peristaltic Pump P-1 (Pharmacia). The column was prepared for ZAC according to the Manufacturer's protocol. See Appendix Section 7.1.3.

After the plasma was loaded, the column was re-equilibrated (1 M NaCl, 20 mM HEPES, pH 7.4) using a Peristaltic Pump P-1.Columns were then attached to an AKTA Pure purification system (GE Healthcare). Loosely bound contaminants were eluted from the column using 15 mM imidazole, 0.5 M NaCl, 20 mM HEPES, pH 7.4. Afterwards, strongly bound proteins including putative α_2M were eluted using from the column using 500 mM imidazole, 0.5 M NaCl, 20 mM

HEPES, pH 7.4. The elution of proteins was monitored using the A_{280} . The collected protein fractions were immediately dialysed in PBS with Az (PBS/Az; 1.37 M NaCl, 27 mM KCl, 100 mM Na_2HPO_4, 18 mM KH_2PO_4, 0.01% (v/v) Az) at 4°C.

Eluted proteins were analysed by SDS and native gel electrophoresis as described in Methods Section 2.2.1 and 2.2.2, respectively.

2.4 Characterization of phenolic compound-modified α_2M

2.4.1 Inducing alternative α_2M conformations.

To induce transformed α_2M conformation, native α_2M was diluted in PBS/Az and treated with 400 mM NH_4Cl. The final concentration of α_2M was ~0.5 mg/ml and the samples were incubated for 2 hours at 37°C.

α_2M was treated with hypochlorite to induce the formation of the dimeric α_2M conformation. Native α_2M was diluted in PBS/Az and treated with either 50 µM or 100 µM NaOCl. The final concentration of α_2M was ~0.5 mg/ml and the samples were incubated overnight at 37 °C. The maximum time proteins were left incubating for was 16 hours.

α_2M was incubated with CA, RA and Saβ, using the same protocol as hypochlorite. The only difference was that α_2M was incubated with either 100 µM or 400 µM of phenolic compound.

2.4.2 Bis-ANS assay

To assess exposed hydrophobic regions on α_2M, a bis-ANS assay was performed. α_2M was diluted in PBS/Az and loading into the wells of a 384-well plate at a concentration of 50 µg/ml. Bis-ANS was diluted in PBS/azide and added to the wells at a final concentration of 10 µM. Solutions were left to incubate for 5 minutes in the dark at room temperature, before endpoint fluorescence of bis-ANS (excitation = 355 nm, emission = 480 nm) was measured using a Clariostar plate reader (BMG Labtech).

2.5 Chaperone Activity involving phenolic compound-modified α_2M

2.5.1 ThT assay

To assess holdase-type chaperone activity of phenolic compound treated α_2M ThT assay was performed using Alzheimer's disease associated amyloid beta peptide ($A\beta_{1-42}$). Prior to performing the ThT assay, α_2M treated with hypochlorite or phenolic compounds were dialysed in PBS/Az at 4°C. Dialysis was performed as both hypochlorite and phenolic compounds have been demonstrated to interact with $A\beta_{1-42}$ to inhibit aggregation of this peptide (Mañucat-Tan *et al*, 2023., Durairajan *et al,* 2008., Tu *et al,* 2018). To ensure the phenolic compounds were removed, samples that contained an equivalent concentration of the phenolic compounds in PBS/Az (without α_2M) were also dialysed and were included in this assay as a dialysis control, abbreviated to DC.

ThT assay was performed on a 384-well plate. The final concentration of samples loaded in the wells was 25 µM ThT and a ratio of 1:40 $A\beta_{1-42}$ to α_2M (10 µM $A\beta_{1-42}$ to 0.25 µM α_2M). Phenolic

compound-DC were loaded at the same volume as their corresponding phenolic compound-modified α_2M samples. For example, RA-α_2M and RA-DC loaded at the same volumes.

The fluorescence of ThT (excitation = 440 nm, emission = 480 nm) was measured in 10 minute intervals using a Clariostar plate reader. Unless otherwise specified, assays ran overnight, with the plate incubated at 28°C and periodically shaken at 300 rpm.

Attempts to optimise conditions for ThT fluorescence of $A\beta_{1-42}$ were made and included different rpms, temperatures, and $A\beta_{1-42}$ concentrations. However, no lag phase was observed in any of the optimisation tests and ThT fluorescence rapidly increased from the very start of every test. Attempts at optimizing the results for $A\beta_{1-42}$ aggregation by slowing rpm, lowering temperature, and decreasing $A\beta_{1-42}$ concentration, did not change this result.

2.6 Cell Surface Binding of phenolic compound-modified α_2M *in vitro*

2.5.1 Recombinant GST-RAP

Receptor-associated protein (RAP) tagged with a glutathione S-transferase (GST) tag (GST-RAP) plasmid was kindly donated by Dr Jordan Cater (University of Wollongong).

2.5.1.1 Transforming chemically competent BL21 *E. coli* cells with GST-RAP plasmid DNA

The chemically competent BL21 *E. coli* cells used in this study were kindly donated by Briony laboratory (Flinders University).

Thawed cells were incubated in ice for 30 minutes with GST-RAP plasmid DNA (50 µg) and subsequently heat-shocked at 42°C for 2 minutes. Then placed back on ice for 5 minutes. Cells were then resuspended in LB broth media (1 ml) and incubated at 37°C for 30 minutes with gentle shaking. Afterwards, cells were centrifuged and the amount of media previous added (1 ml) was removed. Cells were gently resuspended with the remaining supernatant, then spread on LB-agar plates containing ampicillin (see Appendix Section 7.1.4.2) and incubated overnight at 37°C to obtain colonies for further culturing.

2.5.1.2 Inoculation of GST-RAP from transformed BL21 *E. coli* cells

Isolated colonies (see Methods Section 2.5.1.1) were placed in LB broth containing ampicillin and cultured overnight at ~200 rpm. Typically, cells were subcultured at a 1:20 dilution of cells to fresh LB broth containing ampicillin and returned to culture conditions (37°C with shaking at ~200 rpm). The cell density was measured using at the absorbance at 600 nm (OD_{600}) until a reading of between 0.6 to 1.0 was reached. Once optimum optical density was reached, 1 mM of IPTG was added to the cell culture and cells were incubated for another 3 hours to induce GST-RAP expression. Afterwards, the cell culture was pelleted and washed twice in PBS/Az by centrifuge at 4000 x g for 5 minutes. The washed pellets were stored at -80°C.

Thawed pellets were resuspended with lysis buffer (1 mg/ml lysozyme, 0.1 mg/ml DNAse1, 0.1% (v/v) triton X-100, 10mM $MgCl_2$ and EDTA-free complete protease inhibitor cocktail), repeatedly freeze (-170°c)/thawed (+30°c) and subsequently centrifuged at 4000 x g for 20-minutes at 4°c. The supernatant was collected and filtered (0.22 µM).

2.5.1.3 Glutathione affinity chromatography

For glutathione affinity chromatography, 3x 1ml GSTrap HP (GE Healthcare; 3ml total bed volume) was connected in series. Columns were equilibrated with PBS/Az on AKTA Pure.

Filtered supernatant (see Methods Section 2.5.1.2) was loaded into equilibrated columns using a Peristaltic Pump P-1. Loaded columns were re-equilibrated on the Peristaltic Pump P-1 before detaching the columns and once again after the columns were attached to the AKTA Pure.

GST-RAP was eluted from the columns using a buffer containing 10 mM glutathione and 50 mM Tris-HCl. The elution of proteins was monitored using the A_{280}. Protein fractions were immediately dialyzed in PBS/Az at 4°c.

Eluted proteins were analysed by SDS-PAGE under non-reducing conditions, as described in Methods Section 2.2.1. Proteins were also quantified as described in Methods Section 2.2.4.

2.5.2 Mammalian cell culture

All cell cultures were incubated at 37°c in 5% (v/v) atmospheric CO2 under sterile conditions. SH-SY5Y neuroblastoma cells were used in this study. These were grown in medium composed of DMEM-F12 supplemented with 10% (v/v) FBS and 1% (v/v) GlutaMAX. Cells were routinely passaged once a week when 50% to 90% confluent by aspiration of growth media and treatment with 0.05% (w/v) trypsin-EDTA.. Cells were discarded after 20 passages.

2.5.3 Biotinylation of proteins

Proteins were first dialysed in PBS at 4°C, to remove the Az in the samples prior to biotinylating. Proteins were then incubated with 40-fold molar excess of biotin overnight at 4°C with gentle shaking. Proteins were then dialysed in PBS/Az at 4°C. Analysis of by Western blotting (see Methods Section 2.2.3) was performed to confirm proteins were biotinylated.

2.5.4 Flow cytometry

Cells (see Methods Section 2.5.2) were isolated for flow cytometry experiments when 70-90% confluent by incubation with 5 mM EDTA-PBS. The detached cells were washed by centrifugation at 300 x g twice and the cells kept on ice for the duration of the experiment.

For flow cytometry cell were resuspended in Hanks' Balanced Salt Solution (HBSS) containing 0.01% (w/v) BSA (HBSS/BSA) and aliquoted into 1.5 ml tubes, then centrifuged at 300xg for 5 minutes at 4°C to re-pellet cells. Pelleted cells were resuspended with α_2M (50 µg/ml; native, hypochlorite-modified or phenolic compound-modified) diluted in HBSS/BSA and left on ice for 30 minutes before centrifuged again. Alternatively, some cells were treated with 5 µg/ml GST-RAP, which were used as an additional control for cell surface binding. All protein ligands were biotinylated as in 2.5.3. Cells were then resuspended with streptavidin alexa-fluor 488 conjugate (STR-488) diluted with HBSS/BSA at a 1:1000 dilution (STR-488 to HBSS/BSA). Cells were then centrifuged again and resuspended in PBS.

Flow cytometry was performed using a CytoFLEX S (Beckman) to measure fluorescence of bound proteins to cell surface receptors.

3 RESULTS

3.1 Purification of α_2M

α_2M was purified from human plasma using ZAC via established methods. The chromatogram shows that a substantial protein fraction was eluted from the column in the presence of 15 mM imidazole (Figure 4A). This is consistent with the elution of loosely-bound contaminants from the column. A smaller fraction of more tightly-bound proteins was eluted from the column in the presence of 500 mM imidazole (Figure 4A). This smaller protein fraction included putative α_2M. The chromatogram shown is representative of two separate experiments. Proteins eluted from the column by 500 mM imidazole were analysed by SDS-PAGE under non-reducing (Figure 4B) and reducing conditions (Figure 4C). Under non-reducing conditions, the band with a molecular weight above 250 kilo Daltons (kDa) corresponds with the anticipated size of the disulphide-linked α_2M dimer, which is 360 kDa.

In the first attempt to purify α_2M (Lane 1 in Figure 4B and 4C), aside from the band corresponding to the anticipated size of α_2M, there are several additional protein bands present. These bands indicate a notable level of contamination in the sample compared to a subsequent effort to purify α_2M using the same method (Lane 2 in Figure 4B and 4C). Under non-reducing conditions, contaminating protein bands present after the first attempt (Lane 1 in Figure 4B) migrate to two distinct regions that correspond with the expected sizes of human serum albumin (HSA; 66.5 kDa) and immunoglobulins (~150 kDa).

Under reducing conditions, a band corresponding to the anticipated size of the α_2M monomer (180 kDa) was evident in protein fractions obtained from both purification attempts. However, although this band predominated in the protein fractions from the second purification attempt, it constituted only 19% of the protein in the fraction acquired from the initial purification attempt, as determined through densitometry analysis. Due to the notable contamination observed in the protein fraction from the first α_2M purification attempt, this protein was not used for subsequent experiments.

From the initial ~45 ml of blood plasma, the fraction obtained from the second purification attempt yielded a total of 6.28 mg of purified α_2M, as estimated using a nanodrop.

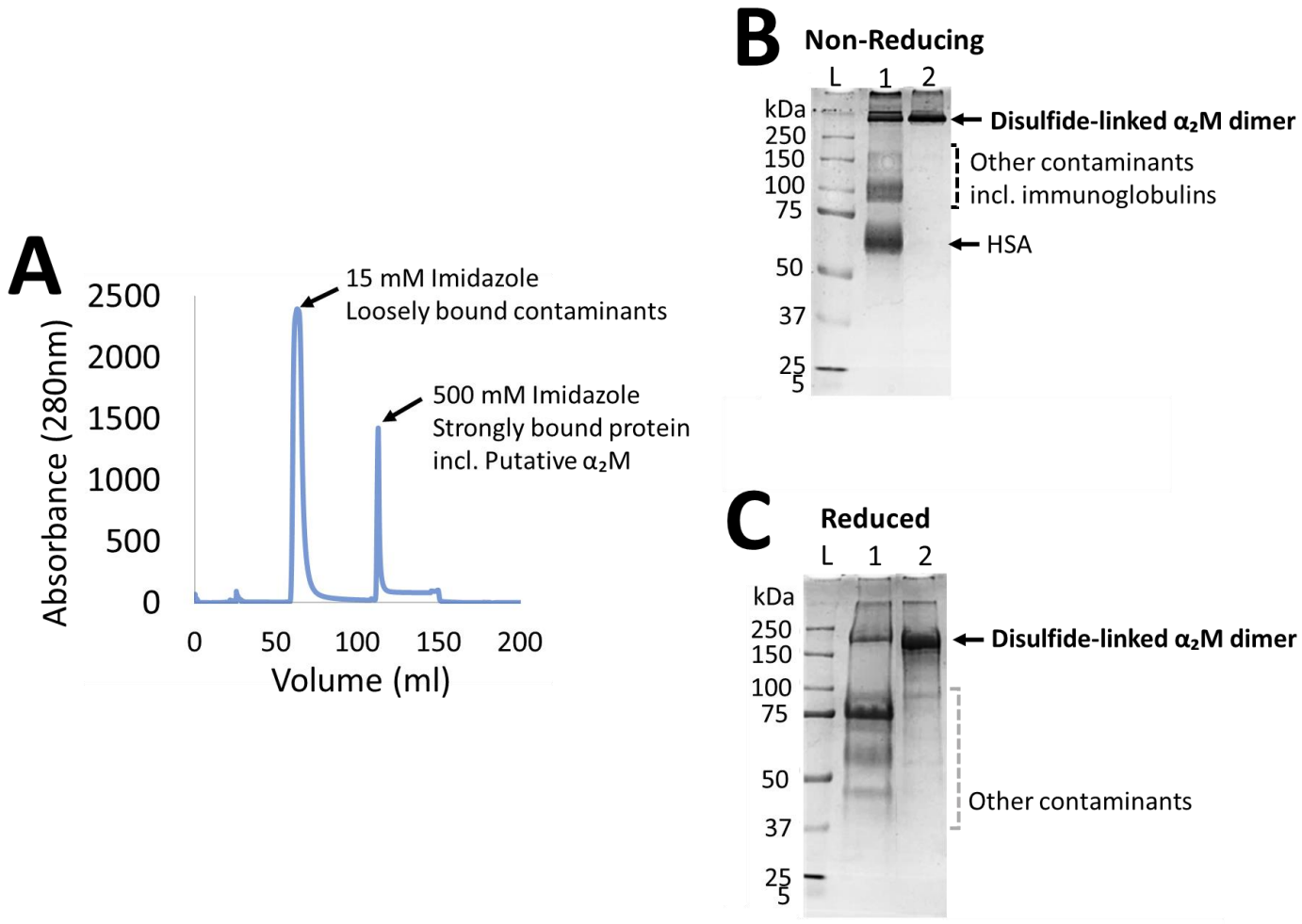

Figure 4. Purification of α_2M from human blood plasma using ZAC. (A) Chromatogram depicting the elution of plasma proteins from a Hitrap chelating HP column prepared for ZAC. Proteins were eluted at a flow rate of 1 ml/min. (B) SDS gel image illustrating proteins eluted by 500 mM imidazole from two attempts to purify α_2M (1 and 2) under nonreducing conditions. (C) Corresponding samples from (A) under reducing conditions. Precision plus protein dual Xtra standards (L; shown in kDa) are included for comparing protein sizes.

3.2 Characterization of phenolic compound-modified α_2M

3.2.1 Native PAGE

Following treatment with phenolic compounds (see Methods Section 2.4.1), the migration pattern of α_2M was examined using native gel electrophoresis. To evaluate the degree of α_2M dissociation, controls such as native α_2M, transformed α_2M (electrophoretically fast), and hypochlorite-modified α_2M were included.

Native α_2M migrated as a single band (Lane 1 in Figure 5). In contrast, α_2M treated with NH_4Clmigrated in two distinct bands. The slightly faster-migrating band corresponded to transformed α_2M, constituting 68% of the protein, as determined by densitometry analysis (Lane 2 in Figure 5). The upper band aligned with native α_2M, representing α_2M tetramers that had not undergone transformation following pre-treatment with NH_4Cl. Hypochlorite-modified α_2M also migrated in two bands, but the faster band was significantly lower on the gel compared to transformed α_2M (Lane 3 in Figure 5). The faster band in the hypochlorite-modified α_2Msample corresponds to dimeric α_2M, which, at 360 kDa, moves more rapidly than tetrameric α_2M (720 kDa) by native gel electrophoresis.

The native gel reveals that incubation with phenolic compounds led to the formation of putative tetrameric and dimeric α_2M species, which migrated similarly but not identically to well-characterized α_2M tetramers and dimers (Figure 5). Specifically, the putative tetrameric species migrated slightly faster than native α_2M but not as fast as transformed α_2M. This difference is particularly evident for proteins treated with 400 µM of phenolic compound, indicating a dose-dependent effect (Lanes 5, 7, and 9 in Figure 5). Similarly, the putative dimeric α_2M, generated

after pre-treatment with phenolic compounds, migrated slightly faster than hypochlorite-modified α_2M dimers. These findings were consistently reproducible across several experiments.

Under the conditions used, the dissociation of α_2M induced by phenolic compounds was only partial, and this effect was observed with all three tested compounds.

Pre-treatment with RA at concentrations of 100 µM and 400 µM (Lanes 4 and 5 in Figure 5) resulted in the dissociation of 16% and 35% of α_2M, respectively, as determined by densitometry. Pre-treatment with CA at 100 µM and 400 µM (Lanes 6 and 7 in Figure 5) resulted in the dissociation of 12% and 21% of α_2M, respectively, while pre-treatment with Saβ at 100 µM and 400 µM (Lanes 8 and 9 in Figure 5) resulted in the dissociation of 9% and 44% of α_2M, respectively. In comparison, pre-treatment of α_2M with 50 µM hypochlorite dissociated approximately 25% of α_2M. Therefore, in terms of inducing α_2M dissociation, in order of potency hypochlorite >> Saβ, RA > CA. In all α_2M samples treated with phenolic compounds, native gel electrophoresis detected small amounts of high molecular weight species (>720 kDa), but these represented less than 5% of the total proteins in all cases (Figure 5).

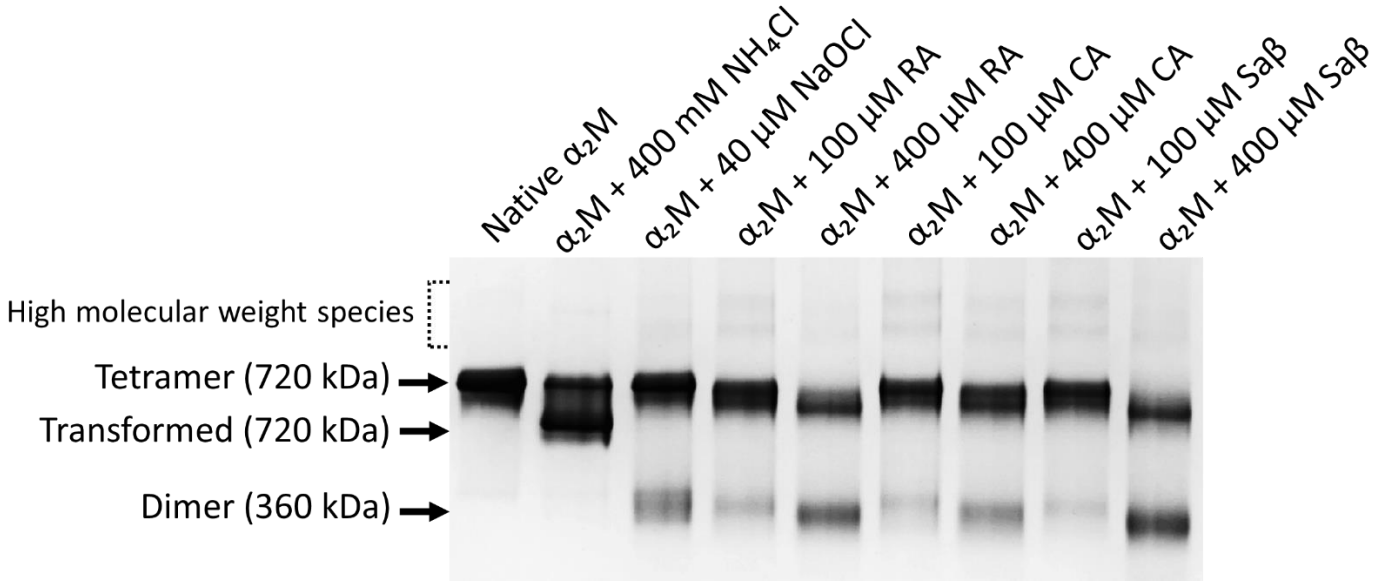

Figure 5. Analysis of α_2M treated with phenolic compounds using Native PAGE. Native α_2M (0.5 mg/ml) was exposed to either 100µM or 400µM RA, CA, or Saβ in PBS overnight at 37°C. (Lane 1) Native α_2M; (lane 2) α_2M treated with 400 mM NH_4Cl; (lane 3) α_2M treated with 50 µM NaOCl; (lane 4) α_2M treated with 100 µM RA; (lane 5) α_2M treated with 400 µM RA; (lane 6) α_2M treated with 100 µM CA; (lane 7) α_2M treated with 400 µM CA; (lane 8) α_2M treated with 100 µM Saβ; (lane 9) α_2M treated with 400 µM Saβ.

3.2.2 Bis ANS assay

To gain deeper insights into the impact of phenolic compound treatment on α_2M, a bis-ANS assay was performed, using native α_2M and hypochlorite-modified α_2M as controls. In line with previously reported findings (Wyatt *et al.*, 2014), treatment with hypochlorite significantly ($P<0.01$) elevated the bis-ANS fluorescence, indicative of increased surface-exposed hydrophobicity in α_2M. However, the results demonstrate that all phenolic compound-modified α_2M preparations had reduced ($P<0.01$) surface-exposed hydrophobicity compared to native α_2M (Figure 6). Specifically, relative to native α_2M, the bis-ANS fluorescence was 5-, 3.5-, and 2.5-

fold lower for α_2M preparations that had undergone pre-treatment with CA, RA, and Saβ, respectively.

When comparing the ability of the three phenolic compounds to reduce surface-exposed hydrophobicity, statistical analysis using one-way ANOVA indicated no significant difference between the effects of the three compounds on bis-ANS fluorescence.

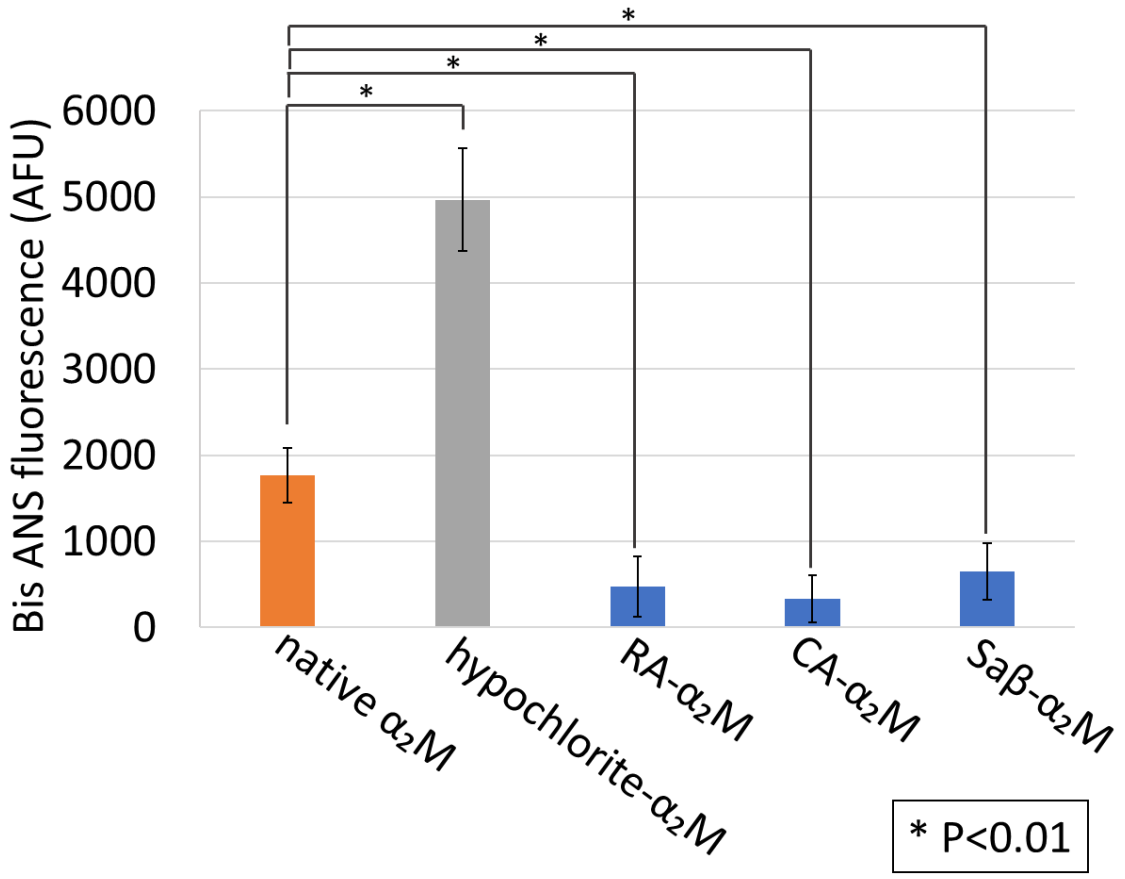

Figure 6. Assessment of exposed surface hydrophobicity in phenolic compound-modified α_2M dimers as measured by bis-ANS fluorescence. The presented data represent the mean bis-ANS fluorescence (AFU) ± SD (n = 10) derived from two independent experiments, with background subtraction (10 µM bis-ANS in PBS) applied to all results and normalization to a starting point of zero. * P<0.01.

3.3 Chaperone Activity of phenolic compound-modified α_2M

3.3.1 ThT assay

The ThT assay was conducted to evaluate the impact of phenolic compounds on the ability of α_2M to inhibit $A\beta_{1-42}$ aggregation *in vitro* (Figure 7). Controls used in this assay included $A\beta_{1-42}$ alone, $A\beta_{1-42}$ incubated with native α_2M, and $A\beta_{1-42}$ incubated with hypochlorite-modified α_2M.

To determine statistical significance, the endpoint ThT fluorescence results were utilized to assess the effectiveness of phenolic compound-modified α_2M in inhibiting Aβ1-42 aggregation compared to the native form (Figure 8).

In this study, Aβ1-42 (in isolation) exhibited rapid aggregation, with no apparent lag phase observed across all replicates. ThT fluorescence began to show signs of stabilization around 400 minutes (6 hours, 40 minutes) (Figure 7). Furthermore, there was notable variability in ThT fluorescence for Aβ1-42, a characteristic that remained consistent throughout the assay. Nevertheless, the results for Aβ1-42 displayed a substantial curve with elevated ThT fluorescence, aligning with the anticipated behavior.

Native α_2M, when incubated with Aβ1-42, displayed a substantial curve akin to Aβ1-42 alone, although with a lower ThT fluorescence measurement (Figure 7). While the mean ThT fluorescence for native α_2M suggested a potential inhibitory effect, there was no statistically significant difference between native α_2M incubated with Aβ1-42 and Aβ1-42 alone, as determined by one-way ANOVA analysis (Figure 8). In line with published research (Wyatt *et al*.,

2014), hypochlorite-modified α_2M, when incubated with Aβ1-42, significantly reduced ThT fluorescence, indicative of its capacity to inhibit Aβ1-42 aggregation (Figure 7).

When CA-α_2M was incubated with Aβ1-42, the ThT fluorescence appeared similar to that of the sample containing native α_2M (Figure 7). However, in contrast to native α_2M, CA-α_2M did show a significant reduction ($P<0.01$) in ThT fluorescence at the end-point of the assay, as determined by one-way ANOVA (Figure 8). This reduction is likely attributed to CA-α_2M exhibiting lower variations in endpoint ThT fluorescence, the point at which statistical analysis was conducted. Notably, while the mean ThT fluorescence for CA-α_2M started to stabilize around 200 minutes (3 hours, 20 minutes), the variability in ThT fluorescence markedly decreased, becoming relatively consistent between replicates around 800 minutes (13 hours, 20 minutes).

Incubation of RA-α_2M with Aβ1-42 led to an initial rise in ThT fluorescence within the first 30 minutes, followed by a gradual decline for the remainder of the assay (Figure 7). Notably, the endpoint ThT fluorescence for RA-α_2M was significantly reduced ($P>0.01$) compared to that of the $A\beta_{1\text{-}42}$ sample containing hypochlorite-modified α_2M (Figure 8). Incubation of Saβ-α_2M with Aβ1-42 also exhibited lower ThT fluorescence compared to the $A\beta_{1\text{-}42}$ sample containing hypochlorite-modified α_2M (Figure 7). However, statistical analysis using one-way ANOVA revealed no significant difference between the ThT fluorescence of the $A\beta_{1\text{-}42}$ samples containing Saβ-α_2M or hypochlorite-modified α_2M at the endpoint of the assay (Figure 8). In comparison, CA-α_2M had the least impact on Aβ1-42 aggregation, resulting in higher ThT fluorescence than Aβ1-42 samples containing either RA-α_2M or Saβ-α_2M at the end-point of the assay ($P<0.01$ and $P<0.05$, respectively) (Figure 8). There was no statistical significance between the ThT

fluorescence of Aβ1-42 samples containing RA-α_2M or Saβ-α_2M at the end-point of the assay, as determined by one-way ANOVA.

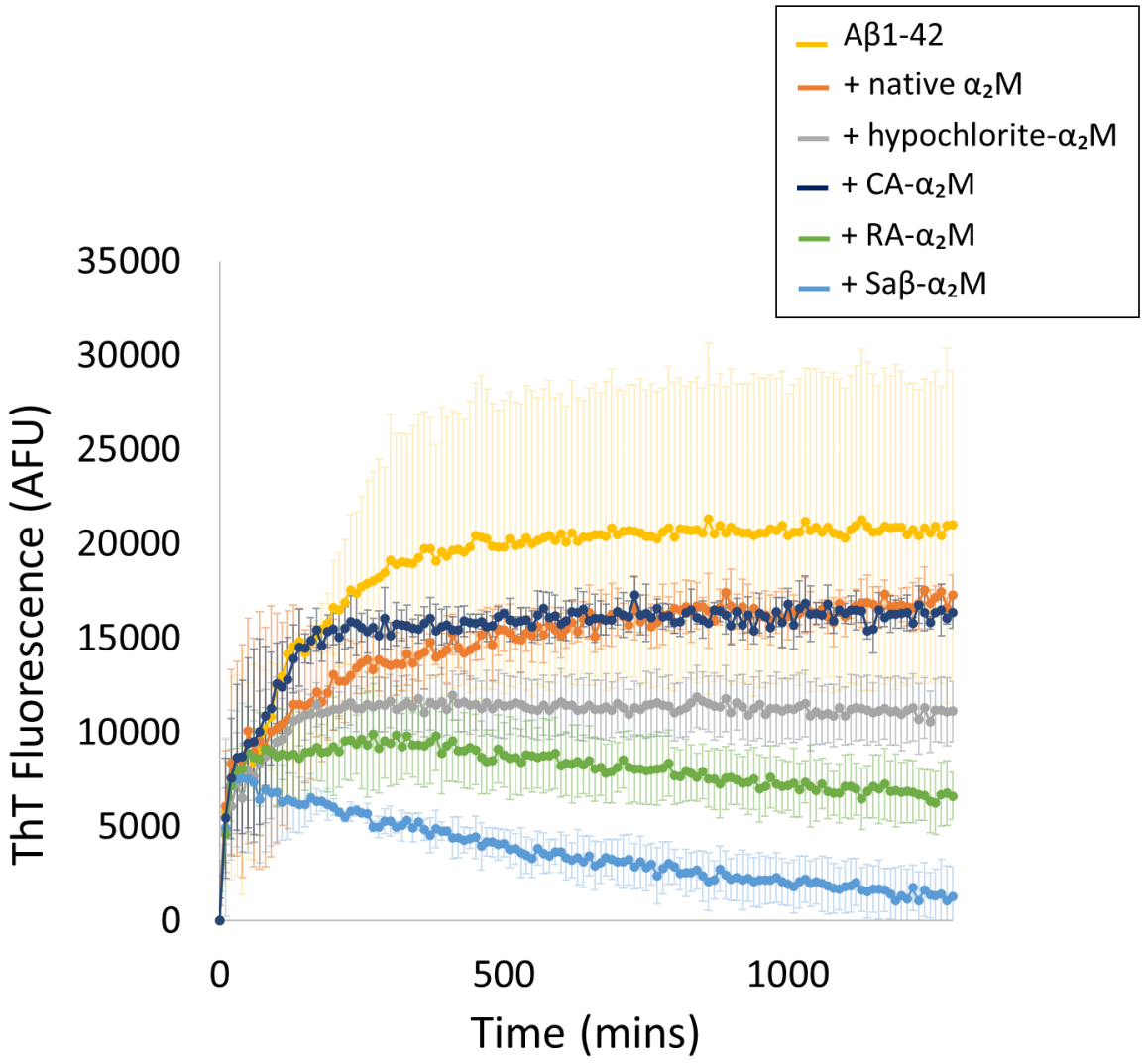

Figure 7. ThT assay illustrating the effect of phenolic compound-modified α_2M on the aggregation of 10µM Aβ_{1-42}. The presented data represent the mean ThT fluorescence (AFU) ± SD (n = 3), with background fluorescence subtracted from all results. Incubation occurred at 28°C with shaking at 300 rpm.

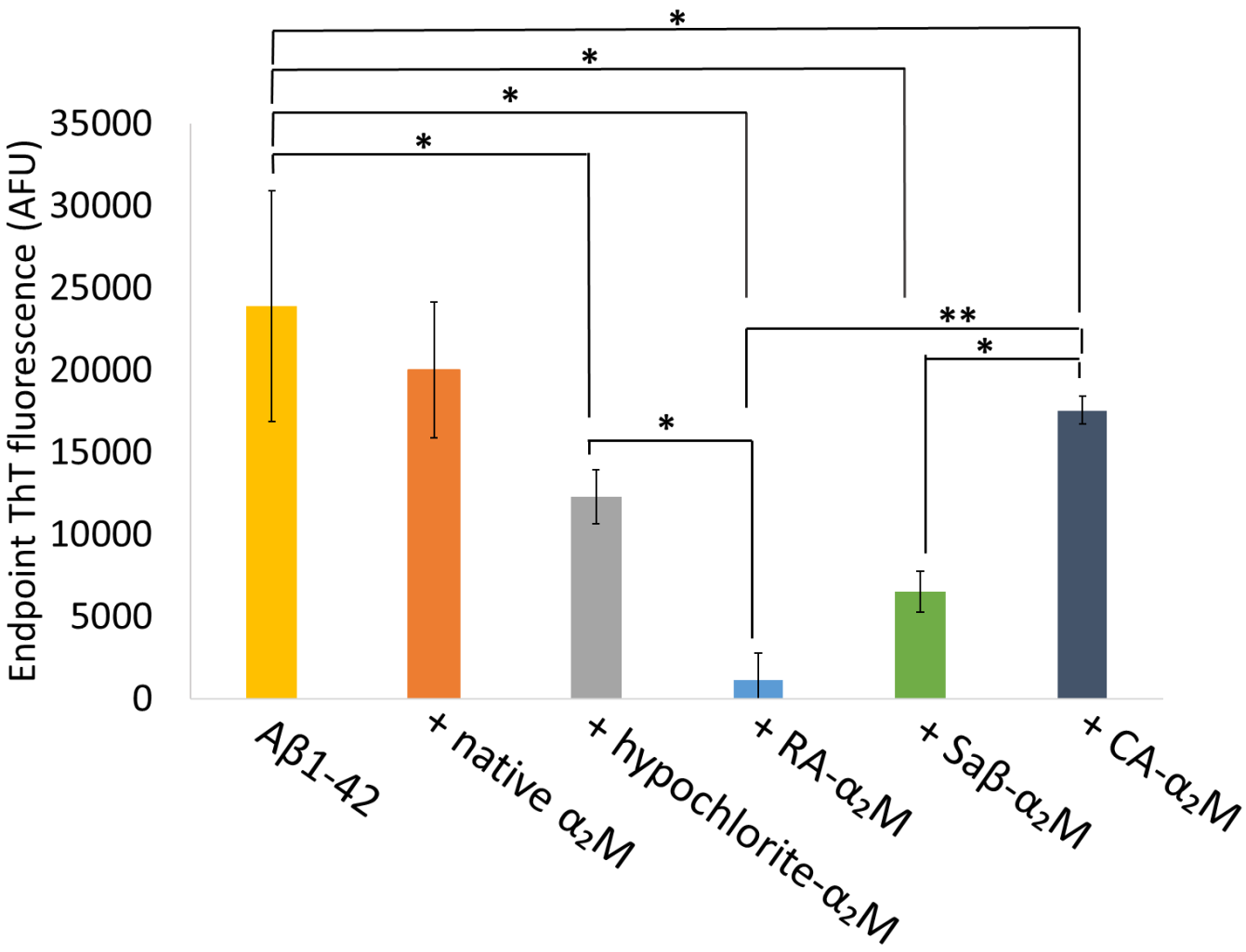

Figure 8. Graph showing the endpoint ThT fluorescence of Aβ1$_{-42}$ incubated in the presence of phenolic compound treated α$_2$M. The ThT fluorescence shown is from the last measurements from each of the phenolic compound-modified α$_2$M from figure 3. The data shown are the mean endpoint ThT fluorescence (AFU) ± SD (n = 3). *P<0.01, **P<0.05.

3.3.1.1 Western blot analysis of endpoint ThT samples

To better understand the results from the ThT assay, endpoint samples were subjected to Western blotting analysis to visualize proteins in the soluble and insoluble fractions (Figure 9). Under these conditions, soluble Aβ1-42 migrated freely through the gel (Lane 1 in Figure 9), while insoluble fibrillar Aβ1-42 couldn't enter the gel and remained in the wells (Lane 2 in Figure 9).

An unexpected observation was the absence of soluble Aβ1-42 in the sample co-incubated with hypochlorite-modified α_2M. Hypochlorite-modified α_2M has previously demonstrated the ability to prevent Aβ1-42 aggregation and maintain its solubility (Wyatt *et al*., 2014). Samples of phenolic compounds in PBS, dialyzed as a control to ensure the removal of phenolic compounds, were also included in both the ThT assay and Western blot analysis (Lanes 4, 6, and 8 in Figure 9). Soluble Aβ1-42 was not detected in any of these samples. Unexpectedly, the sample co-incubated with CA-DC (Lane 8 in Figure 9) lacked detectable Aβ1-42, suggesting a potential error during sample loading.

Interestingly, a band migrating a short distance into the gel (>250 kDa) was detected when Aβ1-42 was co-incubated with phenolic compound-modified α_2M (Lanes 5, 7 and 9 in Figure 9).

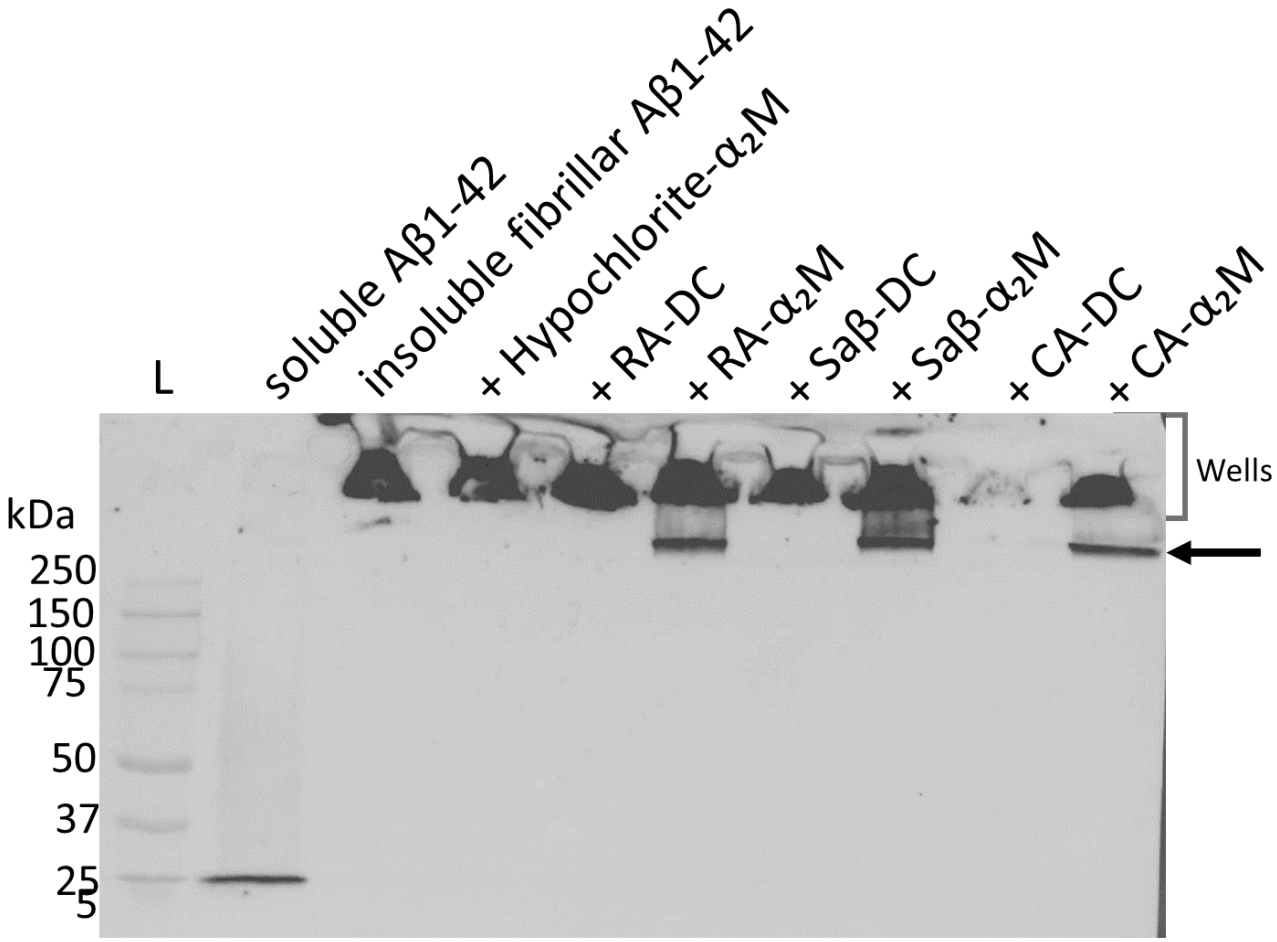

Figure 9. Detection of soluble and insoluble $A\beta_{1-42}$ post ThT assay via Western blot analysis. (Lane 1) Soluble Aβ1-42; (Lane 2) Insoluble fibrillar Aβ1-42; (Lane 3) Co-incubation of hypochlorite-modified α_2M and Aβ1-42; (Lane 4) Co-incubation of RA-DC and Aβ1-42; (Lane 5) Co-incubation of RA-α_2M and Aβ1-42; (Lane 6) Co-incubation of Saβ-DC and Aβ1-42; (Lane 7) Co-incubation of Saβ-α_2M and Aβ1-42; (Lane 8) Co-incubation of CA-DC and Aβ1-42; (Lane 9) Co-incubation of CA-α_2M and Aβ1-42. The arrow indicates the presence of bands where Aβ1-42 has entered the gel. Precision plus protein dual Xtra standards (L; shown in kDa) are included for size comparison of proteins.

3.4 Cell Surface Binding of phenolic compound-modified α_2M *in vitro*

3.4.1 Purification of Recombinant GST-RAP

Recombinant GST-RAP was purified using glutathione affinity chromatography. The chromatogram illustrates a single protein fraction eluted from the column in the presence of 10 mM glutathione (Figure 10A). The protein fraction underwent analysis on SDS-PAGE under non-reducing conditions (Figure 10B).

A distinct band at approximately 67 kDa, corresponds to the expected size of GST-RAP at 64 kDa. Low molecular weight band contaminants, relative to the presumed GST-RAP, are visible around 37 kDa. Additionally, contaminants at 250 kDa and 100 kDa are observable.

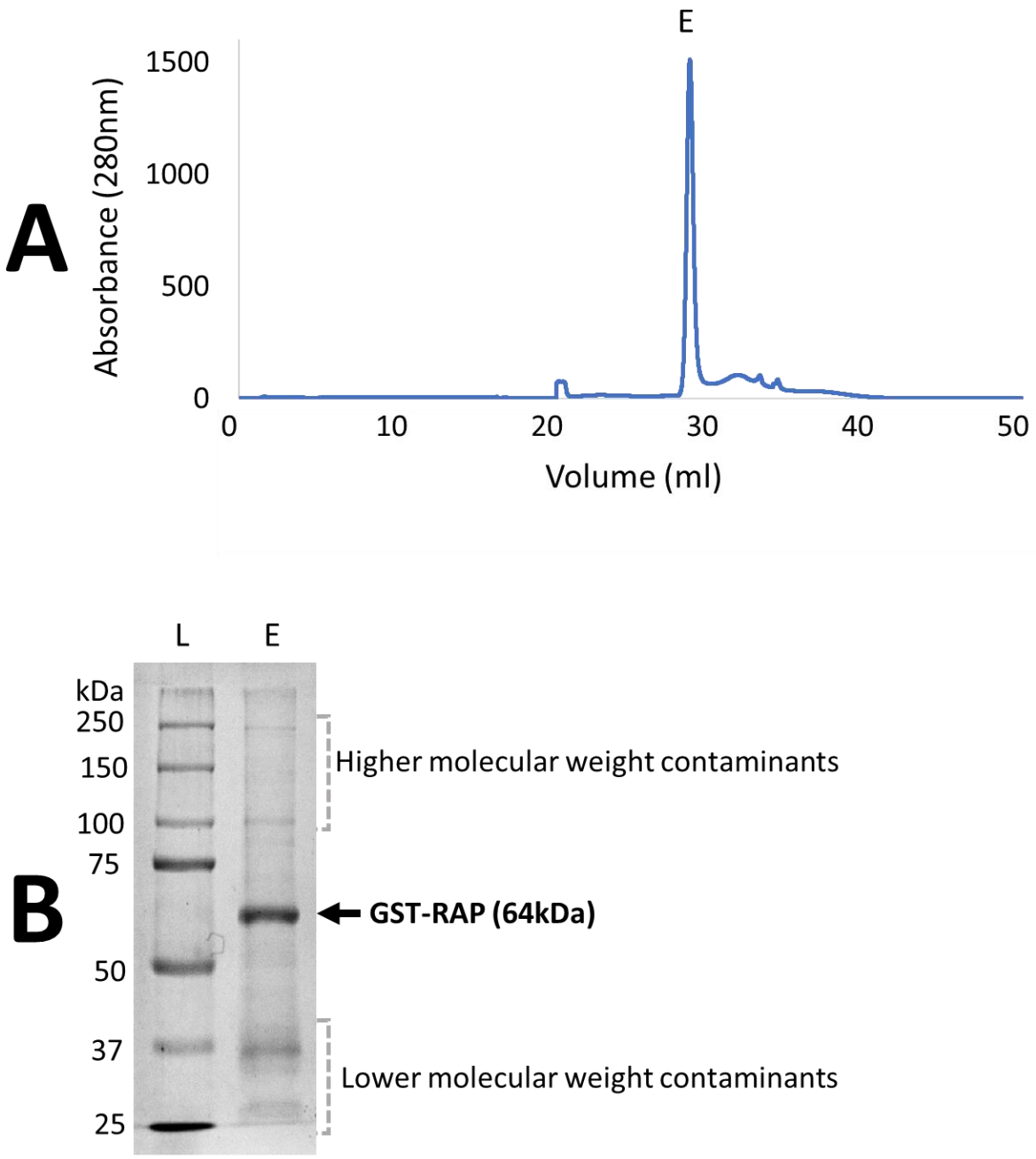

Figure 10. Purification of recombinant GST-RAP by glutathione affinity chromatography. (A) Chromatogram of elution (indicated by E) of GST-RAP from GSTrap HP column at flow rate of 1ml/min. (B) Purified GST-RAP was analysed by SDS-PAGE under non-reducing. Precision plus protein dual Xtra standards (L; shown in kDa) are included for comparison of protein sizes.

3.4.1.1 Western blot analysis of biotinylated GST-RAP

A biotinylated sample of GST-RAP was prepared to facilitate the preliminary investigation of the cell surface binding of phenolic compound-modified α_2M. GST-RAP serves as an appropriate control in this assay because, like transformed and dimeric α_2M, it binds to the LRP-1 cell surface receptor.

Initial evaluation through dot blot analysis with STR-HRP indicated successful biotinylation of the proteins (data not shown). Subsequent Western blotting analysis revealed the presence of lower molecular weight fragments that were also biotinylated (Figure 11).

Due to uncertainties about the purity of GST-RAP and time constraintsr54 K, biotinylated GST-RAP from Demi Georgiou (PhD candidate at Flinders University) was utilized for this study.

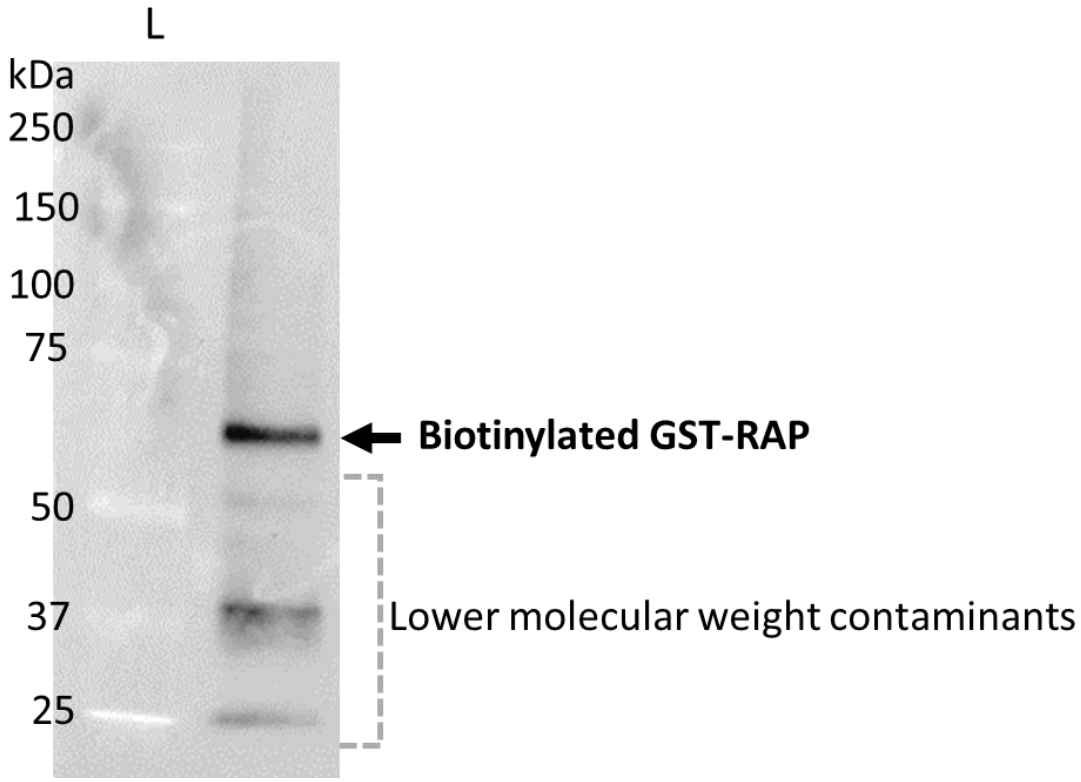

.

Figure 11. Biotinylated GST-RAP analysed by Western blot analysis on SDS-PAGE under nonreducing conditions. Precision plus protein dual Xtra standards (L; shown in kDa) are included for comparison of protein sizes.

3.4.2 Flow cytometry

Preliminary investigations were carried out to examine the binding of biotinylated phenolic compound-modified α_2M to the surface of SH-SY5Y neuroblastoma cells *in vitro*. As mentioned earlier, GST-RAP also binds to this receptor and is therefore utilized as a control for comparing cell surface binding.

The transition of native α_2M into the transformed conformation or dissociated dimer exposes the normally hidden receptor binding site for LRP-1 (Wyatt *et al*., 2014). As expected, pre-incubation

of SH-SY5Y cells with biotinylated native α_2M did not elevate the fluorescence of the cells above the level of the background fluorescence (Graph A in Figure 12). In comparison, pre-incubation of cells with biotinylated hypochlorite-modified α_2M, in which around 50% of the protein was dimeric, increased the measured fluorescence to a level above the background fluorescence, albeit modestly compared to biotinylated GST-RAP (Graph B in Figure 12). Pre-incubation of the cells with biotinylated RA- or Saβ-α_2M increased the fluorescence of the cells compared to the background fluorescence (Graph C and D, respectively, in Figure 12). One-way ANOVA analysis indicated no significant difference between the fluorescence of cells incubated with hypochlorite-, RA-, or Saβ-modified α_2M. Pre-treatment of SH-SY5Y cells with biotinylated GST-RAP resulted in a noticeable shift from the background fluorescence, indicating binding to the surface of the cells (Graph E in Figure 12).

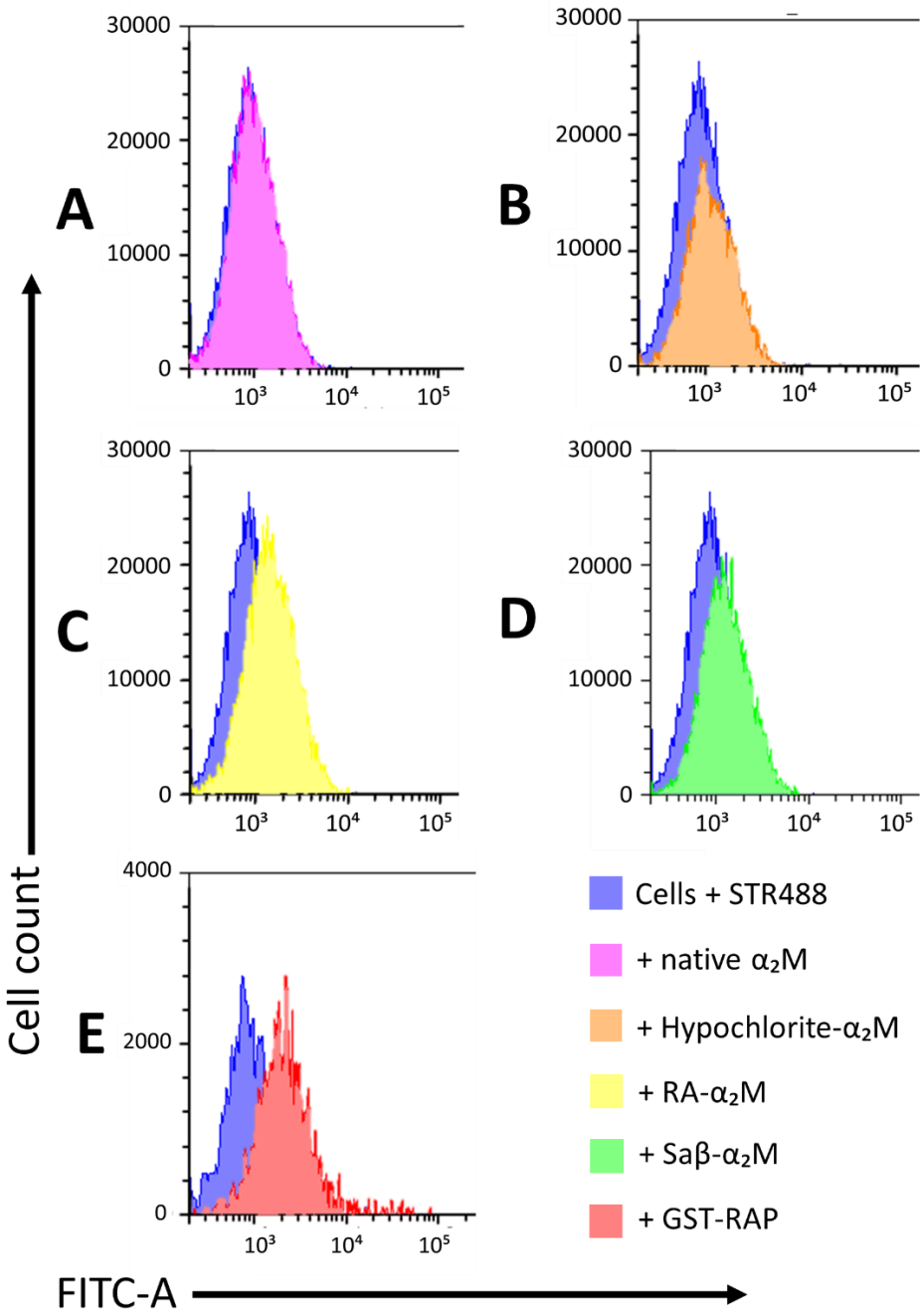

Figure 12. Histograms illustrating the cell surface fluorescence (FITC-A) of SH-SY5Y following incubation with phenolic compound-modified α_2M or controls, as assessed by flow cytometry. The histograms depict the background fluorescence measured after incubating the cells with STR488 alone or biotinylated ligands and STR-488 for the respective treatments: (A) native α_2M, (B) hypochlorite-modified α_2M, (C) RA-α_2M, (D) Saβ-α_2M, and (E) GST-RAP. The results are representative of two independent experiments.

4 DISCUSSION

The results of this study provide proof-of-principle data showing that phenolic compounds can modify the structure and function of α_2M *in vitro*. While it is evident that phenolic compound treatment induces the dissociation of native α_2M into dimer-like molecules, these dimers exhibit substantial differences from those generated by hypochlorite treatment (Wyatt *et al*, 2014).

Currently, there is no published research exploring how phenolic compounds induce the dissociation of α_2M. Nevertheless, investigations involving HSA have revealed that RA interacts at or in proximity to hydrophobic regions of the protein (Peng *et al*, 2016). Furthermore, studies have demonstrated the preferential binding of phenolic compounds, including RA and CA, to Sudlow site I, situated in subdomain IIA of HSA, which is an extensive hydrophobic region (Papaemmanouil *et al*, 2020). The potential binding of phenolic compounds at or near the hydrophobic interface between non-covalently associated disulfide-linked α_2M dimers might provide a plausible explanation for the mechanism by which the dissociation of α_2M is induced.

Notably, the dissociation of α_2M, as induced by phenolic compounds does not lead to an increase in surface hydrophobicity, a characteristic responsible for the heightened chaperone activity of hypochlorite-modified α_2M dimers (Wyatt *et al*, 2014). Instead, treatment of α_2M with phenolic compounds (CA, RA, and Saβ) resulted in a reduction in surface exposed hydrophobicity, even lower than that measured for the native α_2M conformation.

Given that the dissociation between the non-covalently associated disulfide-linked α_2M dimers did not lead to an increase in surface-exposed hydrophobicity, the data supports that the binding

of α_2M to phenolic compounds is also associated with a conformational change that conceals this hydrophobic interface. How this is achieved is not yet known, however, the enhanced electrophoretic motility of phenolic compound-modified α_2M supports the idea that reaction of one or more internal thioester bonds may be induced. Further investigation using DTNB (thiol) assay (Simpson, 2008), would be needed to determine the extent to which this occurs.

Although ThT fluorescence indicated reduced $A\beta_{1-42}$ aggregation when co-incubated with phenolic compound-modified α_2M, free soluble Aβ1-42 was not detected in these samples by Western Blot analysis at the endpoint of this assay. Instead, soluble Aβ1-42 seemed to migrate at the approximate mass of disulfide-linked α_2M supporting the idea that phenolic compound-modified α_2M inhibited Aβ1-42 aggregation by binding to the molecule covalently. The potential exposure of the reactive internal thioester bond in α_2M due to phenolic compound treatment might explain this. Further experiments, such as immunoprecipitation are needed to determine whether or not a stable complex is formed between phenolic compound-modified α_2M and Aβ1-42 under the conditions used.

Since soluble Aβ1-42 was not detected Aβ1-42 when co-incubated with hypochlorite-modified α_2M, which has previously been shown to inhibit Aβ1-42 aggregation via non-covalently binding to the peptide (Wyatt *et al*., 2014), it is possible that soluble Aβ1-42 was present, but not detected in Aβ1-42 samples co-incubated with phenolic compound-modified due to insufficient sample loading or storage of the samples prior to Western blot assay. Analysis of end point samples from ThT assay by transmission electron microscopy would also help to assess the extent to which phenolic compound-modified α_2M inhibits Aβ1-42 fibril formation.

A limitation in the ThT assays performed in this study, is that the phenolic compounds used are known to inhibit Aβ1-42 aggregation in the absence of α_2M (Durairajan *et al,* 2008., Tu *et al,* 2018). Despite extensively dialysing phenolic compound-modified α_2M prior to all assays, it is possible that residual amounts of phenolic compounds remained in the solution. As such, further experiments probing the mechanism by which phenolic compound-modified α_2M reduces Aβ1-42 aggregation should include additional controls to determine the lowest concentration at which phenolic compounds influence Aβ1-42 aggregation independently.

Pre-incubation of SH-SY5Y neuroblastoma cells with α_2M modified by phenolic compounds (RA and Saβ) resulted in a comparable increase in the binding of α_2M to the cell surface, akin to the effect observed with hypochlorite-treated α_2M. This suggests that interaction with phenolic compounds potentially exposes the binding site for LRP-1. However, a limitation of this study is the absence of experiments to specifically determine whether or not the binding of α_2M was mediated by LRP-1 or an alternative mechanism. Due to time constraints, it was not possible to perform experiments involving pre-treatment of the cells with GST-RAP, which is a pan-specific ligand of lipoprotein receptors. Greater insight could also be obtained by treating the cells with an inhibitory anti-LRP-1 antibody (Kerr *et al*, 2010) or performing knock down experiments using siRNA (Taylor and Hooper, 2007). In any case, the preliminary results obtained here support that phenolic compounds may induce a conformational change that reveals the LRP-1 binding site, that is important for the clearance of α_2M and its ligand cargo.

5 CONCLUSION

To date, therapeutic strategies targeting α_2M have largely focused on locally increasing concentrations of the native protein, or generating a pool of transformed α_2M by administering proteases or drugs. This thesis describes the first attempt to used drug-like compounds to induce the dissociation of α_2M into dimers that mirror the functions of hypochlorite-modified α_2M. Surprisingly, although dissociation of α_2M appeared to be an effect of treatment with phenolic compounds, the dimers generated had distinct properties compared to hypochlorite-modified α_2M. Specifically, phenolic compound-modified α_2M did not appear to inhibit Aβ1-42 aggregation via a canonical holdase-type chaperone action involving stabilisation of the peptide in a non-covalent complex. Further investigations are needed in order to fully elucidate the mechanism by which phenolic compound-modified α_2M inhibited Aβ1-42 aggregation and whether phenolic compound modified-α_2M preferentially binds to other disease-associated misfolded protein species. Additionally, due to time limitations it was not possible to investigate the cellular consequences of the binding of phenolic compound-modified α_2M to the surface of cells *in vitro* or to specifically measure the extent to which this is mediated by LRP-1. Further characterisation of the functions of phenolic compound-modified α_2M and identification of compounds that modify α_2M with high specificity and potency may lead to the development of novel therapies for one or more of the many disorders characterised by protein misfolding and/or chronic inflammation.

6 REFERENCES

Albuquerque, B.R., Heleno, S.A., Oliveira, M.B.P., Barros, L. and Ferreira, I.C., 2021. Phenolic compounds: Current industrial applications, limitations and future challenges. *Food & function*, *12*(1), pp.14-29.

Arandjelovic, S., Dragojlovic, N., Li, X., Myers, R.R., Campana, W.M. and Gonias, S.L., 2007. A derivative of the plasma protease inhibitor α2-macroglobulin regulates the response to peripheral nerve injury. *Journal of neurochemistry*, *103*(2), pp.694-705.

Mañucat-Tan, N.B., Chowdhury, A., Cataldi, R., Abdullah, R.Z., Kumita, J.R. and Wyatt, A.R., 2023. Hypochlorite-induced oxidation promotes aggregation and reduces toxicity of amyloid beta 1-42. *Redox Biology*, *63*, p.102736.

Gremmler, L., Kutschan, S., Doerfler, J., Buentzel, J., Buentzel, J. and Huebner, J., 2021. Proteolytic enzyme therapy in complementary oncology: a systematic review. *Anticancer Research*, *41*(7), pp.3213-3232.

Boerger, M., Funke, S., Leha, A., Roser, A.E., Wuestemann, A.K., Maass, F., Bähr, M., Grus, F. and Lingor, P., 2019. Proteomic analysis of tear fluid reveals disease-specific patterns in patients with Parkinson's disease–A pilot study. *Parkinsonism & related disorders*, *63*, pp.3-9.

Bussel, J.B., Vander Haar, E.L. and Berkowitz, R.L., 2021. New developments in fetal and neonatal alloimmune thrombocytopenia. American journal of obstetrics and gynecology, 225(2), pp.120-127.

Cater, J.H., 2021. Investigations of the roles of pregnancy zone protein and plasminogen activator inhibitor type-2 in extracellular proteostasis.

Taylor, D.R. and Hooper, N.M., 2007. The low-density lipoprotein receptor-related protein 1 (LRP1) mediates the endocytosis of the cellular prion protein. *Biochemical Journal*, *402*(1), pp.17-23.

Kerr, M.L., Gasperini, R., Gibbs, M.E., Hou, X., Shepherd, C.E., Strickland, D.K., Foa, L., Lawen, A. and Small, D.H., 2010. Inhibition of Aβ aggregation and neurotoxicity by the 39-kDa receptor-associated protein. *Journal of neurochemistry*, *112*(5), pp.1199-1209.

Cater, J.H., Kumita, J.R., Zeineddine Abdallah, R., Zhao, G., Bernardo-Gancedo, A., Henry, A., Winata, W., Chi, M., Grenyer, B.S., Townsend, M.L. and Ranson, M., 2019. Human pregnancy zone protein stabilizes misfolded proteins including preeclampsia-and Alzheimer's-associated amyloid beta peptide. Proceedings of the National Academy of Sciences, 116(13), pp.6101-6110.

Chiabrando, G., Vides, M. & Sanchez, M. 2002. Differential Binding Properties of Human Pregnancy Zone Protein–and α2-Macroglobulin–Proteinase Complexes to Low-Density Lipoprotein Receptor-Related Protein. Archives of biochemistry and biophysics, 398, 73-78.

Chiabrando, G.A., Vides, M.A. and Sanchez, M.C., 2002. Differential Binding Properties of Human Pregnancy Zone Protein–and α2-Macroglobulin–Proteinase Complexes to Low-Density Lipoprotein Receptor-Related Protein. Archives of biochemistry and biophysics, 398(1), pp.73-78.

Christensen, U., Simonsen, M., Harrit, N. and Sottrup-Jensen, L., 1989. Pregnancy zone protein, a proteinase-binding macroglobulin. Interactions with proteinases and methylamine. *Biochemistry*, *28*(24), pp.9324-9331.

Crookston, K.P., Webb, D.J., Lamarre, J. and Gonias, S.L., 1993. Binding of platelet-derived growth factor-BB and transforming growth factor-β 1 to α2-macroglobulin *in vitro* and *in vivo*: comparison of receptor-recognized and non-recognized α2-macroglobulin conformations. Biochemical Journal, 293(2), pp.443-450.

De Boer, J.P., Creasey, A.A., Chang, A., Abbink, J.J., Roem, D., Eerenberg, A.J., Hack, C.E. and Taylor Jr, F.B., 1993. Alpha-2-macroglobulin functions as an inhibitor of fibrinolytic, clotting, and neutrophilic proteinases in sepsis: studies using a baboon model. *Infection and immunity*, *61*(12), pp.5035-5043.

Di, Y., Han, C., Zhao, L. and Ren, Y., 2018. Is local platelet-rich plasma injection clinically superior to hyaluronic acid for treatment of knee osteoarthritis? A systematic review of randomized controlled trials. Arthritis Research & Therapy, 20(1), pp.1-13.

Durairajan, S.S.K., Yuan, Q., Xie, L., Chan, W.S., Kum, W.F., Koo, I., Liu, C., Song, Y., Huang, J.D., Klein, W.L. and Li, M., 2008. Salvianolic acid B inhibits Aβ fibril formation and disaggregates preformed fibrils and protects against Aβ-induced cytotoxicty. Neurochemistry international, 52(4-5), pp.741-750.

Durairajan, S.S.K., Yuan, Q., Xie, L., Chan, W.S., Kum, W.F., Koo, I., Liu, C., Song, Y., Huang, J.D., Klein, W.L. and Li, M., 2008. Salvianolic acid B inhibits Aβ fibril formation and disaggregates preformed fibrils and protects against Aβ-induced cytotoxicty. *Neurochemistry international*, *52*(4-5), pp.741-750.

Ertugrul, A.S., Sahin, H., Dikilitas, A., Alpaslan, N. and Bozoglan, A., 2013. Evaluation of beta-2 microglobulin and alpha-2 macroglobulin levels in patients with different periodontal diseases. *Australian dental journal*, *58*(2), pp.170-175.

Garton, M.J., Keir, G., Lakshmi, M.V. and Thompson, E.J., 1991. Age-related changes in cerebrospinal fluid protein concentrations. *Journal of the neurological sciences*, *104*(1), pp.74-80.

Geisbrecht, B.V., Lambris, J.D. and Gros, P., 2022, January. Complement component C3: A structural perspective and potential therapeutic implications. In Seminars in immunology (Vol. 59, p. 101627). Academic Press.

Godehardt, A., 2004. *Analyse der Interaktion des GRAB Proteins von S. pyogenes mit α2-Makroglobulin: Einfluss der Interaktion auf die Virulenz und Aufklärung der α2-M Bindungsepitope in GRAB* (Doctoral dissertation).

Gonias, S.L., Oakley, A.C., Walther, P.J. and Pizzo, S.V., 1984. Effects of diethyldithiocarbamate and nine other nucleophiles on the intersubunit protein cross-linking and inactivation of purified human α2-macroglobulin by cis-diamminedichloroplatinum (II). *Cancer research*, *44*(12_Part_1), pp.5764-5770.

Gülçin, İ., 2006. Antioxidant activity of caffeic acid (3, 4-dihydroxycinnamic acid). *Toxicology*, *217*(2-3), pp.213-220.

Harwood, S.L., Diep, K., Nielsen, N.S., Jensen, K.T. and Enghild, J.J., 2022. The conformational change of the protease inhibitor α2-macroglobulin is triggered by the retraction of the cleaved bait region from a central channel. *Journal of Biological Chemistry*, *298*(8).

Harwood, S.L., Nielsen, N.S., Diep, K., Jensen, K.T., Nielsen, P.K., Yamamoto, K. and Enghild, J.J., 2021. Development of selective protease inhibitors via engineering of the bait region of human α2-macroglobulin. *Journal of Biological Chemistry*, *297*(1).

Huang, X., Wang, Y., Yu, C., Zhang, H., Ru, Q., Li, X., Song, K., Zhou, M. and Zhu, P., 2022. Cryo-EM structures reveal the dynamic transformation of human alpha-2-macroglobulin working as a protease inhibitor. *Science China Life Sciences*, *65*(12), pp.2491-2504.

Huang, X., Xi, Y., Pan, Q., Mao, Z., Zhang, R., Ma, X. and You, H., 2018. Caffeic acid protects against IL-1β-induced inflammatory responses and cartilage degradation in articular chondrocytes. *Biomedicine & Pharmacotherapy*, *107*, pp.433-439.

Ikai, A., Ookata, K., Shimizu, M., Nakamichi, N., Ito, M. and Matsumura, T., 1999. A recombinant bait region mutant of human α2-macroglobulin exhibiting an altered proteinase-inhibiting spectrum. *Cytotechnology*, *31*(1-2), pp.53-60.

Jagatia, H. and Tsolaki, A.G., 2021. The role of complement system and the immune response to tuberculosis infection. Medicina, 57(2), p.84.

Janatova, J. and Tack, B.F., 1981. Fourth component of human complement: studies of an amine-sensitive site comprised of a thiol component. *Biochemistry*, *20*(9), pp.2394-2402.

Janssen, B.J., Huizinga, E.G., Raaijmakers, H.C., Roos, A., Daha, M.R., Nilsson-Ekdahl, K., Nilsson, B. and Gros, P., 2005. Structures of complement component C3 provide insights into the function and evolution of immunity. *Nature*, *437*(7058), pp.505-511.

Jourdi, G., Boukhatem, I., Barcelona, P.F., Fleury, S., Welman, M., Saragovi, H.U., Pasquali, S. and Lordkipanidzé, M., 2023. Alpha-2-macroglobulin prevents platelet aggregation induced by brain-derived neurotrophic factor. *Biochemical Pharmacology*, *215*, p.115701.

Kardas, G., Daszyńska-Kardas, A., Marynowski, M., Brząkalska, O., Kuna, P. and Panek, M., 2020. Role of platelet-derived growth factor (PDGF) in asthma as an immunoregulatory factor mediating airway remodeling and possible pharmacological target. Frontiers in pharmacology, 11, p.47.

Kashiwagi, H., Ishimoto, H., Izumi, S.I., Seki, T., Kinami, R., Otomo, A., Takahashi, K., Kametani, F., Hirayama, N., Sasaki, E. and Shiina, T., 2020. Human PZP and common marmoset A2ML1 as pregnancy related proteins. *Scientific Reports*, *10*(1), p.5088.

Kumar, R., Kuligina, E., Sokolenko, A., Siddiqui, Q., Gardi, N., Gupta, S., Varma, A.K. and Hasan, S.K., 2021. Genetic ablation of pregnancy zone protein promotes breast cancer progression by activating TGF-β/SMAD signaling. Breast Cancer Research and Treatment, 185, pp.317-330.

Lee, Y.W., Kim, D.H., Jeon, S.J., Park, S.J., Kim, J.M., Jung, J.M., Lee, H.E., Bae, S.G., Oh, H.K., Son, K.H.H. and Ryu, J.H., 2013. Neuroprotective effects of salvianolic acid B on an Aβ25–35 peptide-induced mouse model of Alzheimer's disease. *European journal of pharmacology*, *704*(1-3), pp.70-77.

Lehmann, G.L., Ginsberg, M., Nolan, D.J., Rodríguez, C., Martínez-González, J., Zeng, S., Voigt, A.P., Mullins, R.F., Rafii, S., Rodriguez-Boulan, E. and Benedicto, I., 2022. Retinal Pigment Epithelium-Secreted VEGF-A Induces Alpha-2-Macroglobulin Expression in Endothelial Cells. Cells, 11(19), p.2975.

Li, Z., Belozertseva, E., Parlakian, A., Bascetin, R., Louis, H., Kawamura, Y., Blanc, J., Gao-Li, J., Pinet, F., Lacy-Hulbert, A. and Challande, P., 2023. Smooth muscle αv integrins regulate vascular fibrosis via CD109 downregulation of TGF-β signalling. European Heart Journal Open, 3(2), p.oead010.

Lin, M., Sutherland, D.R., Horsfall, W., Totty, N., Yeo, E., Nayar, R., Wu, X.F. and Schuh, A.C., 2002. Cell surface antigen CD109 is a novel member of the α2 macroglobulin/C3, C4, C5 family of thioester-containing proteins. *Blood, The Journal of the American Society of Hematology*, *99*(5), pp.1683-1691.

Lin, X., Watanabe, K., Kuragano, M., Kurotaki, Y., Nakanishi, U. and Tokuraku, K., 2020. Dietary intake of rosmarinic acid increases serum inhibitory activity in amyloid a aggregation and suppresses deposition in the organs of mice. *International Journal of Molecular Sciences*, *21*(17), p.6031.

Löb, S., Vattai, A., Kuhn, C., Mittelberger, J., Herbert, S.L., Wöckel, A., Schmoeckel, E., Mahner, S. and Jeschke, U., 2022. The Pregnancy Zone Protein (PZP) is significantly downregulated in the placenta of preeclampsia and HELLP syndrome patients. Journal of Reproductive Immunology, 153, p.103663.

Louis, M.L., Dumonceau, R.G., Jouve, E., Cohen, M., Djouri, R., Richardet, N., Jourdan, E., Giraudo, L., Dumoulin, C., Grimaud, F. and George, F.D., 2021. Intra-articular injection of autologous microfat and platelet-rich plasma in the treatment of knee osteoarthritis: a double-blind randomized comparative study. Arthroscopy: The Journal of Arthroscopic & Related Surgery, 37(10), pp.3125-3137.

Lv, R., Du, L., Zhou, F., Yuan, X., Liu, X. and Zhang, L., 2020. Rosmarinic acid alleviates inflammation, apoptosis, and oxidative stress through regulating miR-155-5p in a mice model of Parkinson's disease. *ACS Chemical Neuroscience*, *11*(20), pp.3259-3266.

Mahmoud, M.A., Okda, T.M., Omran, G.A. and Abd-Alhaseeb, M.M., 2021. Rosmarinic acid suppresses inflammation, angiogenesis, and improves paclitaxel induced apoptosis in a breast cancer model via NF3 κB-p53-caspase-3 pathways modulation. *Journal of applied biomedicine*, *19*(4).

Maurya, D.K. and Devasagayam, T.P.A., 2010. Antioxidant and prooxidant nature of hydroxycinnamic acid derivatives ferulic and caffeic acids. *Food and Chemical Toxicology*, *48*(12), pp.3369-3373.

Michelis, R., Milhem, L., Galouk, E., Stemer, G., Aviv, A., Tadmor, T., Shehadeh, M., Shvidel, L., Barhoum, M. and Braester, A., 2022. Increased serum level of alpha-2 macroglobulin and its production by B-lymphocytes in chronic lymphocytic leukemia. Frontiers in Immunology, 13, p.953644.

Mii, S., Enomoto, A., Shiraki, Y., Taki, T., Murakumo, Y. and Takahashi, M., 2019. CD109: a multifunctional GPI-anchored protein with key roles in tumor progression and physiological homeostasis. *Pathology International*, *69*(5), pp.249-259.

Min, J., Meng-Xia, X., Dong, Z., Yuan, L., Xiao-Yu, L. and Xing, C., 2004. Spectroscopic studies on the interaction of cinnamic acid and its hydroxyl derivatives with human serum albumin. *Journal of Molecular Structure*, *692*(1-3), pp.71-80.

Mortensen, S., Kidmose, R.T., Petersen, S.V., Szilágyi, Á., Prohászka, Z. and Andersen, G.R., 2015. Structural basis for the function of complement component C4 within the classical and lectin pathways of complement. *The Journal of Immunology*, *194*(11), pp.5488-5496.

Nielsen, N.S., Zarantonello, A., Harwood, S.L., Jensen, K.T., Kjøge, K., Thøgersen, I.B., Schauser, L., Karlsen, J.L., Andersen, G.R. and Enghild, J.J., 2022. Cryo-EM structures of human A2ML1 elucidate the protease-inhibitory mechanism of the A2M family. *Nature Communications*, *13*(1), p.3033.

Paciello, F., Di Pino, A., Rolesi, R., Troiani, D., Paludetti, G., Grassi, C. and Fetoni, A.R., 2020. Anti-oxidant and anti-inflammatory effects of caffeic acid: *In vivo* evidences in a model of noise-induced hearing loss. *Food and Chemical Toxicology*, *143*, p.111555.

Papaemmanouil, C., Chatziathanasiadou, M.V., Chatzigiannis, C., Chontzopoulou, E., Mavromoustakos, T., Grdadolnik, S.G. and Tzakos, A.G., 2020. Unveiling the interaction profile of rosmarinic acid and its bioactive substructures with serum albumin. Journal of Enzyme Inhibition and Medicinal Chemistry, 35(1), pp.786-804.

Petersen, C.M., 1993. Alpha 2-macroglobulin and pregnancy zone protein. Serum levels, alpha 2-macroglobulin receptors, cellular synthesis and aspects of function in relation to immunology. Danish medical bulletin, 40(4), pp.409-446.

Reddy, V.Y., Desorchers, P.E., Pizzo, S.V., Gonias, S.L., Sahakian, J.A., Levine, R.L. and Weiss, S.J., 1994. Oxidative dissociation of human alpha 2-macroglobulin tetramers into dysfunctional dimers. *Journal of Biological Chemistry*, *269*(6), pp.4683-4691.

Shao, J., Jin, Y., Shao, C., Fan, H., Wang, X. and Yang, G., 2021. Serum exosomal pregnancy zone protein as a promising biomarker in inflammatory bowel disease. Cellular & Molecular Biology Letters, 26(1), pp.1-13.

Simpson, R.J., 2008. Estimation of Free Thiols and Disulfide Bonds Using Ellman's Reagent. CSH protocols, 2008, pp.pdb-prot4699.

Solomon, K.R., Sharma, P., Chan, M., Morrison, P.T. and Finberg, R.W., 2004. CD109 represents a novel branch of the α2-macroglobulin/complement gene family. Gene, 327(2), pp.171-183.

Sottrup-Jensen, L., Sand, O., Kristensen, L. and Fey, G.H., 1989. The α-macroglobulin bait region: Sequence diversity and localization of cleavage sites for proteinases in five mammalian α-macroglobulins. *Journal of Biological Chemistry*, *264*(27), pp.15781-15789.

Sun, C., Cao, C., Zhao, T., Guo, H., Fleming, B.C., Owens, B., Beveridge, J., McAllister, S. and Wei, L., 2023. A2M inhibits inflammatory mediators of chondrocytes by blocking IL-1β/NF-κB pathway. Journal of Orthopaedic Research®, 41(1), pp.241-248.

Tariq, S., Mirza, M.R., Choudhary, M.I., Sultan, R. and Zafar, M., 2022. Prediction of Type 2 diabetes at pre-diabetes stage by mass spectrometry: a preliminary study. *International Journal of Peptide Research and Therapeutics*, *28*(4), p.111.

Tavassoli, M., Janmohammadi, N., Hosseini, A., Khafri, S. and Esmaeilnejad-Ganji, S.M., 2019. Single-and double-dose of platelet-rich plasma versus hyaluronic acid for treatment of knee osteoarthritis: A randomized controlled trial. World Journal of Orthopedics, 10(9), p.310.

Troeberg, L. and Nagase, H., 2012. Proteases involved in cartilage matrix degradation in osteoarthritis. *Biochimica et Biophysica Acta (BBA)-Proteins and Proteomics*, *1824*(1), pp.133-145.

Tu, L.H., Tseng, N.H., Tsai, Y.R., Lin, T.W., Lo, Y.W., Charng, J.L., Hsu, H.T., Chen, Y.S., Chen, R.J., Wu, Y.T. and Chan, Y.T., 2018. Rationally designed divalent caffeic amides inhibit amyloid-β fibrillization, induce fibril dissociation, and ameliorate cytotoxicity. European Journal of Medicinal Chemistry, 158, pp.393-404.

Tu, L.H., Tseng, N.H., Tsai, Y.R., Lin, T.W., Lo, Y.W., Charng, J.L., Hsu, H.T., Chen, Y.S., Chen, R.J., Wu, Y.T. and Chan, Y.T., 2018. Rationally designed divalent caffeic amides inhibit amyloid-β fibrillization, induce fibril dissociation, and ameliorate cytotoxicity. European Journal of Medicinal Chemistry, 158, pp.393-404.

Tu, L.H., Tseng, N.H., Tsai, Y.R., Lin, T.W., Lo, Y.W., Charng, J.L., Hsu, H.T., Chen, Y.S., Chen, R.J., Wu, Y.T. and Chan, Y.T., 2018. Rationally designed divalent caffeic amides inhibit amyloid-β fibrillization, induce fibril dissociation, and ameliorate cytotoxicity. *European Journal of Medicinal Chemistry*, *158*, pp.393-404.

Varma, V.R., Varma, S., An, Y., Hohman, T.J., Seddighi, S., Casanova, R., Beri, A., Dammer, E.B., Seyfried, N.T., Pletnikova, O. and Moghekar, A., 2017. Alpha-2 macroglobulin in Alzheimer's disease: a marker of neuronal injury through the RCAN1 pathway. *Molecular psychiatry*, *22*(1), pp.13-23.

Wang, S., Wei, X., Zhou, J., Zhang, J., Li, K., Chen, Q., Terek, R., Fleming, B.C., Goldring, M.B., Ehrlich, M.G. and Zhang, G., 2014. Identification of α2-macroglobulin as a master inhibitor of cartilage-degrading factors that attenuates the progression of posttraumatic osteoarthritis. *Arthritis & rheumatology*, *66*(7), pp.1843-1853.

Webb, D.J. and Gonias, S.L., 1998. A modified human alpha 2-macroglobulin derivative that binds tumor necrosis factor-alpha and interleukin-1 beta with high affinity *in vitro* and reverses lipopolysaccharide toxicity *in vivo* in mice. *Laboratory investigation; a journal of technical methods and pathology*, *78*(8), pp.939-948.

White, R., Janoff, A. and Godfrey, H.P., 1980. Secretion of alpha-2-macroglobulin by human alveolar macrophages. Lung, 158(1), pp.9-14.

Wu, S.M., Patel, D.D. and Pizzo, S.V., 1998. Oxidized α2-macroglobulin (α2M) differentially regulates receptor binding by cytokines/growth factors: implications for tissue injury and repair mechanisms in inflammation. The Journal of Immunology, 161(8), pp.4356-4365.

Wyatt, A.R., Kumita, J.R., Mifsud, R.W., Gooden, C.A., Wilson, M.R. and Dobson, C.M., 2014. Hypochlorite-induced structural modifications enhance the chaperone activity of human α2-macroglobulin. Proceedings of the National Academy of Sciences, 111(20), pp.E2081-E2090.

Xiao, X., Cai, W., Ding, Z., Shi, Y., Fan, L. and Zhang, Q., 2023. A2M Serves as Promising Biomarker for Chronic Obstructive Pulmonary Disease. International Journal of Chronic Obstructive Pulmonary Disease, pp.683-692.

Zaitone, S.A., Ahmed, E., Elsherbiny, N.M., Mehanna, E.T., El-Kherbetawy, M.K., ElSayed, M.H., Alshareef, D.M. and Moustafa, Y.M., 2019. Caffeic acid improves locomotor activity and lessens inflammatory burden in a mouse model of rotenone-induced nigral neurodegeneration: Relevance to Parkinson's disease therapy. *Pharmacological Reports*, *71*, pp.32-41.

Zhang, H.F., Wang, Y.L., Gao, C., Gu, Y.T., Huang, J., Wang, J.H., Wang, J.H. and Zhang, Z., 2018. Salvianolic acid A attenuates kidney injury and inflammation by inhibiting NF-κB and p38 MAPK signaling pathways in 5/6 nephrectomized rats. *Acta Pharmacologica Sinica*, *39*(12), pp.1855-1864.

Zhu, M., Zhao, B., Wei, L. and Wang, S., 2021. Alpha-2-macroglobulin, a native and powerful proteinase inhibitor, prevents cartilage degeneration disease by inhibiting majority of catabolic enzymes and cytokines. Current Molecular Biology Reports, 7, pp.1-7.

Zia, M.K., Siddiqui, T., Ali, S.S., Ahsan, H. and Khan, F.H., 2018. Interaction of anti-cancer drug-cisplatin with major proteinase inhibitor-alpha-2-macroglobulin: Biophysical and thermodynamic analysis. *International journal of biological macromolecules*, *116*, pp.721-727.

7 APPENDICES

7.1 Methods and Protocols

7.1.1 SDS-PAGE Hand cast 8% tris-HCl SDS gel

Hand cast gels involved the preparation of an 8% resolving polyacrylamide gel solution (total volume prepared of 10mL; 4.6 mL MilliQ H2O, 2.7 mL 30% (w/v) Acrylamide:Bisacrylamide (37.5:1), 2.5 mL Tris (1.5 M, pH 8.8), 0.1 mL 10% (w/v) SDS, 0.1 mL 10% (w/v) ammonium persulfate and 0.006 mL TEMED), with 7ml of the gel solution poured into 1.5 mm-spaced glass plates in a Mini-PROTEAN Tetra Cell casting system. This was immediately followed by pipetting 90% ethanol on top of the gel solution and allowing it to set for 15 minutes. Once set, the ethanol was rinsed out with MilliQ H2O. A 5% stacking gel solution was prepared (Total volume prepared of 5mL; 2.8 mL MilliQ H2O, 0.67 mL 30% (w/v) Bis-acrylamide, 0.5 mL Tris (1.0 M, pH 6.8), 0.04 mL 10% (w/v) SDS, 0.04 mL 10% (w/v) ammonium persulfate, with 0.004 mL TEMED) and was poured on top of stacking gel with a 10-well comb inserted and allow to set (~15mins)

7.1.2 AKTA Protocol

For glutathione-agarose affinity chromatography, zinc affinity chromatography (ZAC) and size exclusion chromatography (SEC) an AKTA Pure (GE Healthcare) was used. All buffers used on the AKTA system were filtered using a vacuum filter (0.22µm filter membrane) and degassed using a Elmasonic P (Elma) for 60-minutes.

Before attaching columns, the system was washed with MilliQ (flow rate 5-10ml/min) until A280 had stabilised and subsequently equilibrated according to manufacturer specifications of the column (flow rate 5-10ml/min). The AKTA was paused between changing of buffers.

Columns were attached at a flow rate of 0.5ml/min and flow rate were increased according to column recommended specifications.

7.1.3 loading proteins onto columns

A peristaltic pump was used to load syringe filtered (0.22µm) protein samples onto columns for purification. Prior to loading, the tubing of the pump was washed (MilliQ) and equilibrated according to manufacturer specifications running at an approximate flow rate of 3ml/min for 5-minutes. The flow rate was slowed to the minimum setting for connecting the columns and flow rate was then increased to 1ml/min for loading of protein samples. Proteins samples were on ice during loading. Once sample were loaded, the columns were re-equilibrated at the flow rate of 1ml/min for 15-minutes. Flow rate was slow to minimum setting for disconnection of columns. Once removed, 0.1M NaOH was flushed through the tubing at a flow rate of 1ml/min for about 10-minutes. Tubing was then washed with MilliQ and 20% ethanol at a flow rate of 3ml/min before the pump was turned off (filled with 20% ethanol).

7.1.4 Dialysis

Immediately after elution of proteins by chromatography, proteins were dialysed in PBS/0.01% (w/v) sodium azide at 4°c. Dialysis tube or cup used floated in a buffer volume of 2L to 5L. Buffer

wash change after a 2-hour (repeated twice) before left overnight. After dialysis, proteins were collected and stored at 4°c.

7.1.5 GST-RAP

7.1.5.1 Preparation of reagents, buffers and culture plates

LB Broth

12.5g Broth base powder was dissolved with MilliQ to a final volume of 500ml. The dissolved solution was Autoclaved on at 121°c for 20-minutes. Autoclaved LB broth was stored at room temperature (sealed) until use.

Ampicillin stock

Ampicillin stocks were prepared at a concentration of 50mg/ml from ampicillin sodium salts. Ampicillin sodium salts (2g) were dissolved in MilliQ to a final volume of 20ml. The ampicillin solution was filtered use a 0.22µm syringe filter under sterile conditions. After filtering,1ml aliquotes were made and stored at -20°c.

Agar culture plates with ampicillin

10g of LB agar powder was dissolved in MilliQ to a final volume of 250ml. The dissolved solution was Autoclaved on at 121°c for 20-minutes. Working under sterile conditions, Ampicilin was

incorporated into the agar solution at a concentration of 100µg/ml. The Agar solution was then poured into sterile petri dishes to about halfway and left to dry (with lid on). Dry petri dishes were sealed with parafilm and placed (inverted) in a bag that was then sealed. Plates were stored at 4°c until use.

Lysis Buffer

200mg Lysozyme (1mg/ml), four EDTA-free complete protease inhibitor cocktail, 0.4066g MgCl·6H2O, 20mg DNAse 1 (0.1mg/ml) and 200µl triton X-100 (0.1% v/v) was combined in MilliQ at a final volume of 200ml. This was stored at 4°c until use.

7.1.5.2 Upscale protocol and Incoulation of GST-RAP from transformed BL21 *E. coli* cells

Isolated single colonies from were collected using the end of a pipette tip, with the tip dropped into 5ml of LB broth containing ampicillin (in a 50ml flask) and cultured overnight (~16 hours) at 37°c with shaking at 200 rpm in an orbital mixer incubator (RAKET). The next day the 5ml of cell culture was poured into a 2L flask and the volume was adjusted to 250ml with overnight culture condition repeated.

After the second overnight culture, the optical density at a wavelength of 600nm (OD_{600}) was measured (optimal between 0.6 to 1.0) and the cells were subculture using fresh LB broth containing ampicillin (100µg/ml), so that OD_{600} was approximately 0.2. In this case, 200mL of

cultured cells were added to a 6L flask and the volume adjusted to 4L. The cells were incubated again at 37°c with shaking at 200 rpm) and where OD_{600} was monitored every hour until measuring between 0.6 to 1.0. Once optimum optical density was reached, 1mM of IPTG (0.953g) was added to the cell culture and cell were incubated for another 3-hours to induce GST-RAP expression. Afterwards, the cell culture was centrifuged at 4000xg for 5-minutes using a Multifuge X Pro Series centrifuge (Thermo Fisher Scientific) and the supernatant was removed. A total of six 250ml centrifuge flasks () were used. This required the cell culture to be added to flask, centrifuged, resuspended with new cell culture and re-centrifuged at least 2x per flask before cells were finally pelleted and a wash step performed. The pellets were washed in PBS/0.01% (w/v) sodium azide twice by centrifuging at 4000xg for 5 minutes. The washed pellets were stored at -80°c.

The next day the pellets were thawed on ice and resuspended with lysis buffer at a final volume of 40ml. The resuspended pellets were freeze (-170°c, liquid nitrogen)/thawed (37°c, incubator) three times and subsequently centrifuged at 4000xg for 20-minutes at 4°c. The supernatant was collected, and syringe filtered using 0.22µm).

7.1.6 Cryopreservation of SH SY5Y cells

For cryopreservation, low passage-number cell lines (50% confluent) were suspended in freezing medium (50% (v/v) FCS, 40% (v/v) DMEM/F-12, 10% (v/v) dimethyl sulfoxide) and aliquoted into sterile cryogenic vials, which were immediately transferred to a Mr. Frosty freezing container (Thermo Fisher Scientific) in a −80°C freezer.

The frozen cells were transferred to liquid N2 for long term storage.

7.2 Standard curve for determining kDa of GST-RAP.

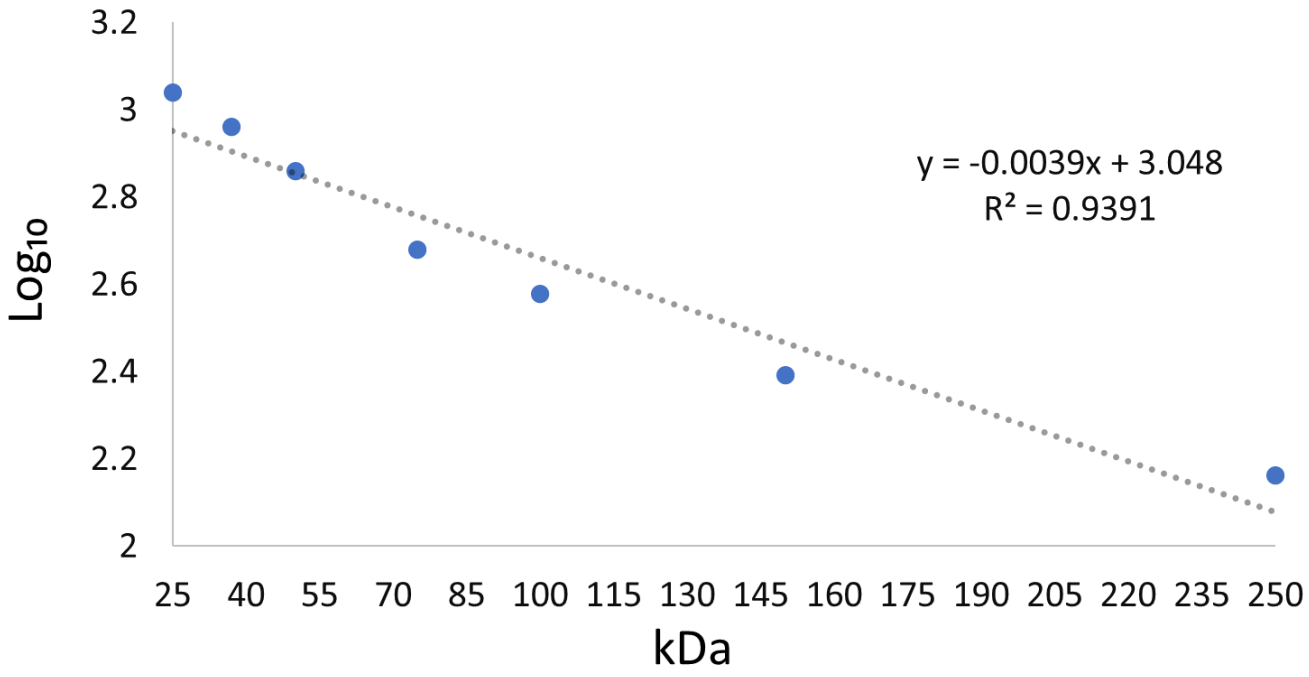

Figure 13. Standard curve of kDa distance from GST-RAP SDS-PAGE. Distance of ladder were measured on the SDS image and converted to log. Linear equation shown on graph.